

## 1

## Synthesis of Hairy Nanoparticles

Zongyu Wang<sup>1</sup>, Jiajun Yan<sup>1,2</sup>, Michael R. Bockstaller<sup>1</sup>, and Krzysztof Matyjaszewski<sup>1</sup>

<sup>1</sup>Carnegie Mellon University, Department of Chemistry, 4400 Fifth Avenue, Pittsburgh, PA 15213, USA

<sup>2</sup>ShanghaiTech University, School of Physical Science and Technology, 393 Middle Huaxia Road, Shanghai 201210, China

### 1.1 Introduction to Grafting Chemistry

Recent progress in the field of macromolecular science affords economically feasible materials with mechanical robustness, light weight, and advanced optical, thermal, or electronic transport performance to impact fields, such as energy storage, transportation, electronics, and bioengineering. Hybrid materials that derive novel and enhanced properties from the synergisms between distinct organic and inorganic (or biological) constituents play a particularly important role. Research in this area is often inspired by “nature” that employs multifunctional hybrid materials (such as “mollusk shells”) in which novel properties arise due to the hierarchical arrangement of constituents. An important theme is the role of interfaces in mediating the interactions between the constituents. Surface functionalization via anchored polymer chains has become a ubiquitously applied method to tune the physiochemical properties of the surface, leading to significant improvements in interface chemistry and engineering [1–11]. Advances in surface-initiated polymerization have enabled the synthesis of brush (or “hairy”) nanoparticles, a novel class of hybrid material “building blocks” that can be assembled into functional material architectures or that can be applied as fillers to augment the performance of polymer materials. The incorporation of nanoparticles allows for enhancing the performance of the polymer host without sacrificing the superior processability features of the host matrix. The ability to construct polymeric materials with defined or desired thermal, optical, catalytic, electronic, and mechanical performance rendered the so-called polymer nanocomposites one of the most active fields in modern macromolecular chemistry and engineering. Applications of brush particles to realize stimuli-responsive polymer hybrids [2, 8, 12, 13], antifouling paints [5, 14–16], colloidal stabilizers [17], adhesives [18], catalytic systems [19], electronic devices [20], and biosensors [21] have been demonstrated. Moreover, hairy nanoparticles prepared via surface-initiated polymerization have

found application for the functionalization of various novel substrates, including nanofibers, mesoporous constituents, nanotubes, graphene, living cells, and protein nanocomposites [22–25]. This contribution summarizes recent advances in the field of surface-initiated polymerization, in particular, based on reversible-deactivation polymerization methods, that have been fundamental to the advances in polymer hybrid materials [10, 26, 27].

## 1.2 Surface Functionalization of Nanoparticles

The preparation of hairy nanoparticles starts with the introduction of functional groups onto nanoparticle surfaces to enable the subsequent coupling of polymer chains (“grafting-onto” approach) or initiating groups for surface-initiated polymerization (“grafting-from” approach). The generation of strong bonding between the polymer chains and inorganic substrates surface relies on the precise and proper selection of desired anchoring groups.

### 1.2.1 Surface Modification by Chemical Treatment

A large number of anchoring reagents with distinct functionalities were explored to fulfill the surface modification of the respective desired substrates. Table 1.1 includes some general functional groups and their suitable surfaces. Examples of anchoring reagents and the applicable functional groups are summarized and listed below. One of the most commonly used reagents for surface functionalization is silane-based coupling agents, as many commercially available functional silanes, including trimethoxy(vinyl)silane, (3-aminopropyl)triethoxysilane, (3-mercaptopropyl)trimethoxysilane, and (3-chloropropyl)triethoxysilane, are available at a low price from the industrial sources. The introduced amino moieties are subsequently converted to different functionalities, including atom transfer radical polymerization (ATRP) initiating sites. Many other functionalities can also be incorporated through hydrosilylation reactions. The silanol group on the surface can react with the functional groups. Silane-based coupling agents can consume up to three halide or alkoxy functional groups. Hence, the anchoring reagent with multiple functionalities can form a stronger covalent bond to the surface of nanoparticles. However, the multifunctional silane coupling agents tend to self-polymerize and form a multilayered microstructure [60]. The construction of the multilayered structure empowers the coupling agents with functional groups to enclose the surface, therefore making them widely applicable to a broad range of substrates.

Pyrocatechol, also known as catechol, and its derivatives have attracted great attention in the past years [34, 61]. Pyrocatechol, especially dopamine or polydopamine, was originally recognized to assemble stable adhesion to the surfaces of metal oxide substrates by forming a chelate attachment [62]. Nevertheless, the breakthrough of dopamine-like peptides in the byssus of mussels expanded the application of (poly)dopamine as a universal surface modifier. Generally, dopamine self-polymerizes into a multilayered polydopamine covering the substrate [34]. The

**Table 1.1** Surface anchoring groups and applicable surfaces.

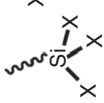
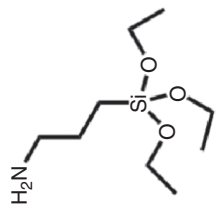
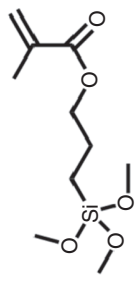
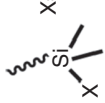
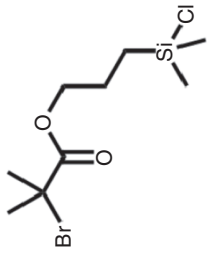
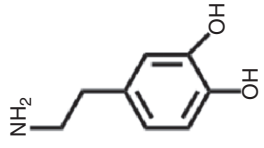
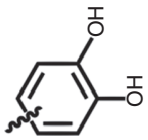
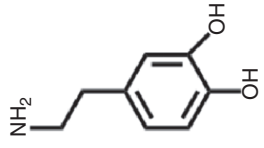

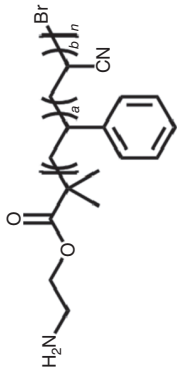

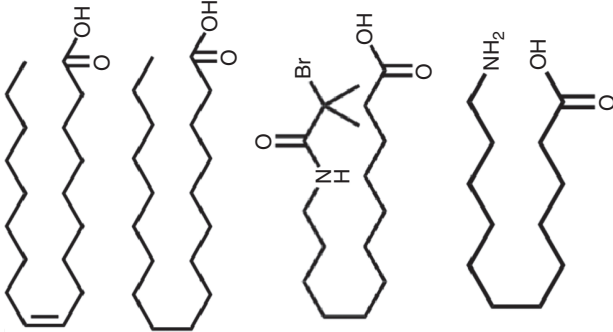
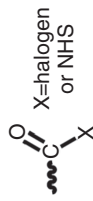
Anchoring group	Surface	Examples	References
Trihalo/alkoxysilane  X=halogen or RO	Silica, metal oxide, metal, etc.	 	[28–31]
Halo/alkoxydimethylsilane  X=halogen or RO	Silica	 	[32, 33]
Catechol 	Metal, metal oxide, carbon, etc.		[34–37]

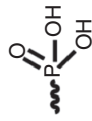
Table 1.1 (Continued)

Anchoring group	Surface	Examples	References
Amino  $R=H$ or $CH_3$	Metal, metal oxide, carboxylic acid-functionalized surface		[38]
Carboxylic acid 	Metal, metal oxide, amino-functionalized surface		[39–42]

Activated acyl

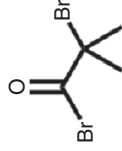


Phosphonic acid/  
phosphates



Radical

Hydroxy/amino-functionalized  
surface, cellulose



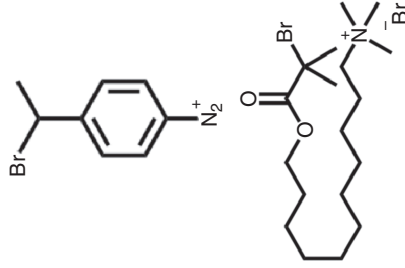
[43-45]

Metal oxide



[46, 47]

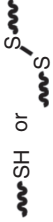
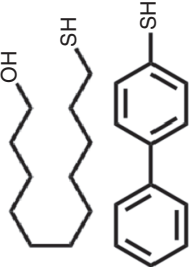



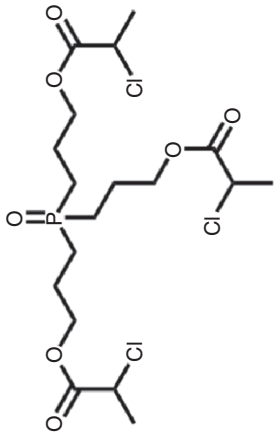
Metal, metal oxide, carbon



[48-50]

---

Table 1.1 (Continued)

Anchoring group	Surface	Examples	References
Thiol/disulfide 	Metal		[51–56]
Allyl 	Hydrogen-treated silicon		[32]
Phosphine oxide 	Quantum dots		[57, 58]

Source: Yan et al. [59], table 1 (p. 198)/Reproduced with permission from Elsevier.

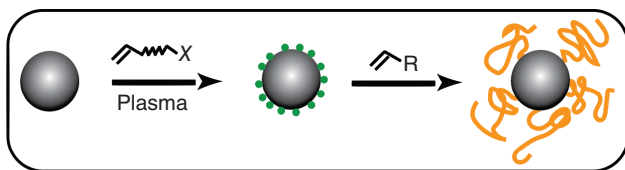
formation of polydopamine affords a large variety of surface functional groups, such as amino, hydroxyl, aromatics, and conjugated carbonyl [61, 63, 64]. Besides dopamine, other natural and synthetic compounds based on phenol/catechol were employed as anchoring reagents, including catechol-bearing peptides and tannic acid [65, 66].

The application of aliphatic acids to the functionalization of metal or metal oxide surfaces has been well explored in the field of inorganic surface modification [67]. Later, aliphatic acids, or amines, were utilized to stabilize inorganic colloid nanocrystals in organic dispersion [68–70]. Either carboxyl or amino groups can generate coordinative interaction with the metal atoms on the surfaces [70–72]. Nevertheless, low-cost aliphatic acids or amines, including oleic acid, stearic acid, octylamine, or dodecylamine, initially served simply for compatibilization with no reactive functional groups incorporated. Recent research proved the introduction of ATRP initiating sites or even polymer chains with carboxylic acid or amino chain ends onto the nanofiller surfaces [38, 39]. A carboxylate-based anchor showed high efficiency to modify a large variety of inorganic substrates. The incorporation of ATRP initiating moieties allowed the application of these anchoring reagents for the synthesis of hybrid polymer nanocomposite [39, 73]. Besides aliphatic acids or amines, another alternative approach to modify the surface of the inorganic substrate is the deposition of aniline or pyrrole [74]. However, their control over the surface functionality as well as the anchoring efficiency is not as facile as silane or dopamine coupling agents [75]. The hydroxyl- or amino-modified surfaces can directly react with the coupling agents based on derivatives of carboxylic acids, including acyl halide or active esters [43, 44, 76]. Compared to carboxylic acids, as one alternative surface anchoring agent, functional phosphonates and phosphates were used to graft polymer chains onto/from salts and metal oxides as they can build strong bond with the surface of metal oxide substrates [46, 77, 78]. Phosphine oxides functionalized the surface of selective quantum dots, including cadmium selenide or zinc sulfide [57, 58]. Additionally, radical species generated through heat, light, or redox reaction from the surface or precursors introduced functional moieties and formed covalent carbon–carbon/metal bonds on the substrate surfaces. For instance, thermal initiators attached to the surface of carbon substrates upon heating [79]; aryl radicals were produced through the electrochemical reduction of diazonium compounds [48, 80, 81]; and radical coupling with alkenes yields photochemically active surfaces [82, 83]. Similar to the typical process of radical coupling, hydrosilylation can connect allyl-based anchoring reagents and pretreated silicon substrates through either a thermal/photoinduced radical path or an organometallic catalytic path [32]. Organosulfur compounds can form a stable linkage with a wide range of metals, including gold, silver, mercury, iron, or copper. In these systems, thiols and disulfides were efficiently anchored to the metal surface, providing proper coupling functionalities. For instance, thiols are commonly employed to tune the size of gold nanoparticles [84]. Disulfides were prone to split into thiolates upon chemisorption on metal surfaces [85, 86]. Initiating sites or polymer ligands were incorporated onto surfaces of gold via coordination with compounds containing

mercapto groups or thiol-terminated polymer ligands [51–53]. The essence of the sulfur–metal interaction is still under investigation [86, 87].

### 1.2.2 Surface Modification by Plasma Treatment

Plasma is a moderately ionized vapor of free electrons, ions, and radicals. It can be defined as a quasi-neutral particle system in the form of a gaseous or fluid-like blend [88–91]. During plasma treatment, functional groups are immobilized onto the surfaces or free radicals are produced. The radicals can react with oxygen from the atmosphere and be used for subsequent coupling or grafting reactions [92]. Gases such as argon, helium, oxygen, nitrogen, ammonia, and carbon tetrafluoride are particularly widely applied. The anchored moieties can further be used to bind other molecules or polymers to the surface to afford the targeted properties. For example, oxygen plasma treatment induced oxygen-containing functionalities including hydroxyl groups, peroxide groups, and carboxyl groups. Carboxyl and hydroxyl groups may also be incorporated via carbon dioxide or CO-plasma treatment [93]. The carbon dioxide plasma treatment creates ketones, aldehydes, and esters [94]. Nitrogen, ammonia, and nitrogen/hydrogen plasmas produce primary, secondary, and tertiary amines, and amides, which can be used to initiate polymerization in the postirradiation grafting procedure [95]. The pulsed plasma treatment can entail the deposition of halogen-containing initiator films on the surface of the substrate (Scheme 1.1) [96–98].

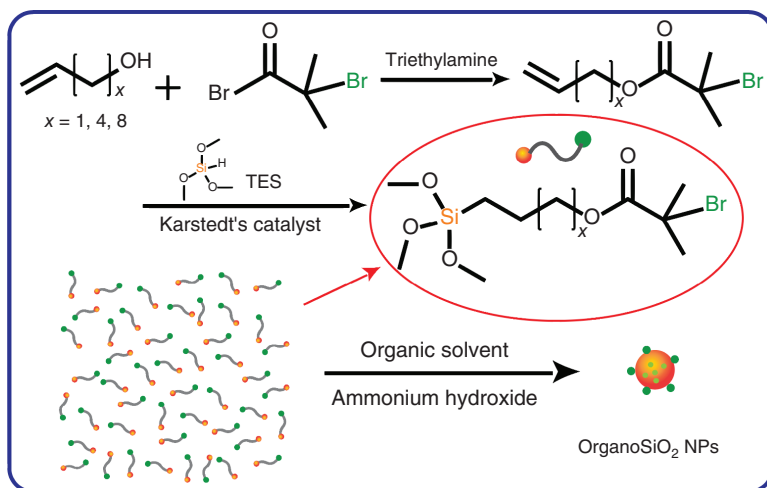


**Scheme 1.1** Surface-initiated polymerization from pulsed plasma deposited halogen-containing initiator layers.

### 1.2.3 Synthesis of Functionalized Nanoparticles Through Initiator-Containing Precursors

Instead of tethering the initiators onto the nanoparticle surfaces, a one-step process to prepare uniform 3 nm initiator-containing organo-silica hybrid nanoparticles was reported [99], which relied on the polycondensation of brominated organosilane precursors, 3-(triethoxysilyl)alkyl  $\alpha$ -bromoisobutyrate (TES-ABMP). The utilization of an initiator-modified precursor enabled one to spare the surface modification steps prior to polymerization, hence avoiding the generation of additional silica layers from coupling reactions. In Scheme 1.2, “green Br” refers to the bromine initiating sites that are essential for synthesizing the hairy nanoparticles, and “x” indicates the number of  $-\text{CH}_2-$  units, which are attributed to preparing the corresponding organosilane precursor. The hybrid nanoparticles can readily be polymer-tethered through surface-initiated atom transfer radical polymerization (SI-ATRP) without additional post-functionalization [6].





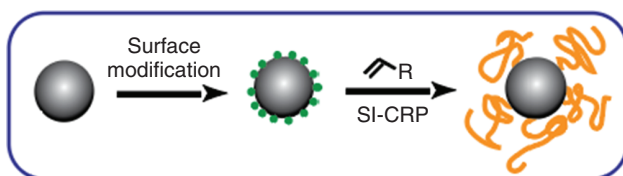
**Scheme 1.2** Synthesis of  $\text{oSiO}_2$  nanoparticles. Source: Han et al. [99], scheme 1 (p. 1219)/Reproduced with permission from the American Chemical Society.

### 1.3 Synthesis of Hairy Nanoparticles

In the past decades, numerous methodologies and techniques have been explored for polymer–inorganic hybrid material synthesis. Modification of inorganic substrates with tethered polymer ligands optimally integrates the properties of both ingredients [100]. Polymer ligands could be synthesized either by “grafting-from” or “grafting-onto” approaches [101–103]. The “grafting-onto” method exploits the benefits of coupling reactions between the surface functionalities and the complementary anchoring blocks or (chain ends) of polymer ligands to be attached to the substrate surfaces [104], which is experimentally straightforward. On the other hand, the “grafting-from” modification is often preferred as it enables higher grafting densities and polymer shell thicknesses. Both the “grafting-onto” and “grafting-from” approaches involve reactions at a solid surface. In an alternative approach, hairy nanoparticles were synthesized through a “polymer-first” approach, for instance, by applying block copolymers as a template [105]. This procedure was further advanced to prepare covalently bonded hairy nanoparticles with more complicated morphologies, including nano-capsules [106], molecular bottlebrushes [107–109], and star polymers [110], as polymeric templates to prepare precisely controlled polymer–inorganic nanocomposites.

#### 1.3.1 Surface-Initiated Polymerization/The “Grafting-from” Approach

In the “grafting-from” method (Scheme 1.3), tethered polymer ligands grow directly from the modified surfaces, enabling higher grafting density, which is one of the most significant advantages of this approach. The grafting density (unit: chains  $\text{nm}^{-2}$ ) of hairy nanoparticles is defined as the average number of polymer chains per unit surface area (unit:  $\text{nm}^2$ ) and represents a crucial parameter for tuning both the chemical and physical properties of brush-like composites.



**Scheme 1.3** The “grafting-from” approach.

### 1.3.1.1 SI-Free Radical Polymerization

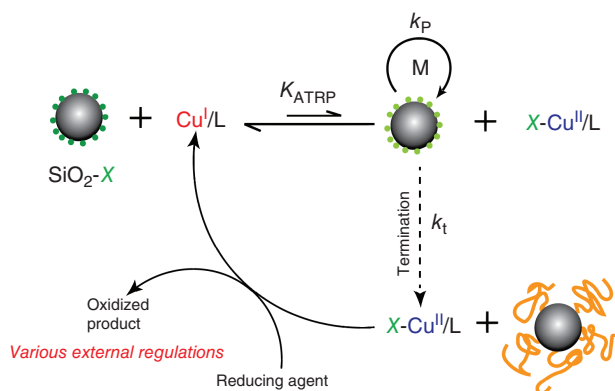
Conventional (free) radical polymerization (FRP) is the most industrially utilized polymerization technique [111]. It has a long history of grafting polymer brushes from inorganic particles [112, 113]. To perform SI-FRP from nanoparticles, a radical-generating moiety needs to be immobilized. Radicals may be generated via conventional azo initiators [113, 114], photoinitiators [115, 116], or ionizing irradiations [117, 118]. Similar to FRP in solution, surface-generated radicals undergo radical addition to vinyl monomers and the reaction proceeds via a chain-growth mechanism. The multifunctional nature of the nanoparticle “macroinitiators” allows the growth of multiple chains simultaneously on a single nanoparticle.

FRP is one of the least expensive polymerization techniques while it is compatible with the widest variety of vinyl monomers. It is also tolerant to many impurities, such as protic solvents (e.g. water or alcohol), coordinating/chelating agents, and electrophiles, and various polymerization conditions, including bulk, solution, suspension, and (mini/micro)emulsion polymerization [119]. SI-FRP inherits all these features.

Despite such advantages, its intrinsic limitations render SI-FRP a nonideal choice in the preparation of hairy nanoparticles. Due to the high frequency of diffusion-controlled random termination reactions, broad molecular weight distribution is virtually guaranteed for FRP. It may not be a problem for homogeneous systems, but with several hundred growing chains on each nanoparticle, such random distribution leads to a large particle-to-particle difference, and hence a large batch-to-batch difference, as well as gelation due to radical termination between particle brushes.

### 1.3.1.2 SI-ATRP

In FRP it is challenging to simultaneously optimize each parameter of the targeted materials, particularly when the polymerization of the tethered chains is carried out from surfaces. The advances in surface-initiated controlled radical polymerization (SI-CRP), also known as surface-initiated reversible deactivation radical polymerization (SI-RDRP), allow precise control over chain length, composition, brush shell thickness, and eventually polymer architecture at the same time. They afford an approach to modify various substrates with polymeric shells of different thicknesses meanwhile maintaining the robustness and versatility of the living polymerization technique. The high tolerance of SI-CRP as a synthetic method toward a wide variety of functionalities and extensive applicability enabled it to be broadly applied for the fabrication of hairy nanoparticles.

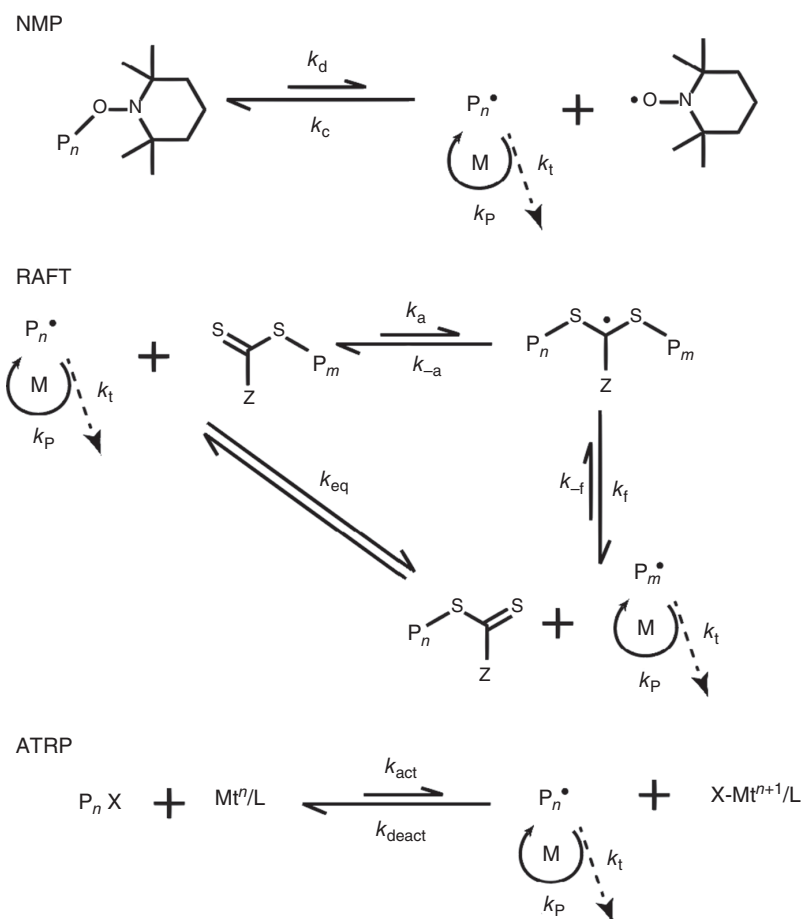


**Scheme 1.4** General scheme for SI-ATRP.

Because of the high accessibility of alkyl halide functional groups on the surface and its high tolerance toward various reaction environments, process requirements, and impurities, SI-ATRP amounts to a majority of all “grafting-from” approaches (Scheme 1.4). SI-ATRP as well as its derivative techniques have been recognized as the most common controlled radical polymerization (CRP) approach for growing polymer ligands from substrate surfaces [4, 6, 10, 120], substantially augmenting the toolkit of radical polymerization. SI-ATRP with well-preserved chain-end fidelity was employed for the preparation of precisely controlled, densely tethered polymer ligands from colloidal nanocrystals [120–122]. Based on the dynamic equilibrium between propagating radicals and dormant species, a typical ATRP procedure is tempered by a redox pair of transition metal complex catalysts, especially copper complexes ( $\text{Cu}^{\text{I}}/\text{L}$ ,  $\text{Cu}^{\text{II}}/\text{L}$ ), Figure 1.1 [123–126]. A conventional ATRP process typically includes initiation, propagation, activation/deactivation, and termination steps, similar to SI-ATRP. However, the heterogeneous system presents some special characteristics.

Determined by the diverse morphology of nanoparticles and the degree of surface functionalization, the density of initiating sites could vary in a wide range, up to a couple thousand per particle, resulting in hairy nanoparticles with a very high grafting density. To achieve good control throughout the process, the overall rate of the polymerization should be well-tuned to maintain a sufficient diffusion rate of monomers to the chain-end radicals.

Additionally, when the overall number of initiating sites or deactivators is not high enough, then reversible deactivation becomes too slow, and extra sacrificial initiators [127] or deactivators [110] are added to the reaction to maintain a sufficiently fast reversible deactivation to enable a controlled process. Besides, based on the general gelation theory, for functionalized particles containing a thousand initiating sites on the surface, just about 0.1% of interparticle couplings could result in macroscopic gelation [128]. Reagents containing  $\alpha$ -bromoisobutyrate functional groups are commonly used to introduce initiating sites on the surface of nanoparticles for SI-ATRP. Recent work reported the development of a tetherable ATRP initiator, 12-( $\alpha$ -bromoisobutyramido)dodecanoic acid (BiBADA), which contains a long



**Figure 1.1** Illustration of equilibrium of typical RDRP techniques.

aliphatic spacer between a carboxyl group and an  $\alpha$ -bromoisobutyramido chain end. Due to its versatility, BiBADA was used as a universal anchor for the surface modification of metal oxide nanoparticles (Table 1.2, Figure 1.2).

For some applications, the residual catalysts from SI-ATRP should be separated from the ultimate product. In the past decades, numerous methodologies were exploited to afford a precisely controlled polymerization with only ppm levels of copper complex catalyst. Reducing agents were employed to restore the activator of copper complexes with high reactivity, such as Cu/Me<sub>6</sub>TREN or Cu/TPMA [129]. There are examples utilizing chemical reducing agents, including activator regenerated by electron transfer (ARGET) ATRP [130, 131], supplemental activator and reducing agent (SARA) ATRP [132, 133], and initiator for continuous activator regeneration (ICAR) ATRP [134]. Later, external stimuli [135], for instance, electrochemical method [136, 137], photo-irradiation [138, 139], and ultrasound agitation [140–143], were applied to produce the reducing environments (Figure 1.3). These methods not only enabled ppm levels of copper complex catalyst

**Table 1.2** Summary of polymer-grafted metal oxide nanoparticles synthesized by SI-ATRP using BiBADA.<sup>a)</sup>

	Entry	Particle	Size (nm)	Monomer	$M_n^b$	$M_w/M_n^b$	$\sigma$ (nm <sup>-2</sup> ) <sup>c)</sup>	$D_h$ (nm) <sup>d)</sup>
Alkaline earth	1	MgO	20	MMA	$1.32 \times 10^5$	1.60	0.08	$1600 \pm 200$
Transition metal	2	TiO <sub>2</sub>	15	MMA	$7.24 \times 10^4$	1.25	0.03	$403 \pm 5$
	3	Co <sub>3</sub> O <sub>4</sub>	10–30	MMA	$1.03 \times 10^5$	1.83	0.14	$4800 \pm 100$
	4 <sup>e)</sup>	NiO	10–20	MMA	$7.69 \times 10^4$	1.28	0.14	$236 \pm 3$
	5	ZnO	18	MMA	$8.77 \times 10^4$	1.33	0.17	$282 \pm 1$
	6	Y <sub>2</sub> O <sub>3</sub>	10	MMA	$1.66 \times 10^5$	1.72	0.24	$650 \pm 10$
	7	ZrO <sub>2</sub>	40	MMA	$5.56 \times 10^4$	1.52	0.15	$236 \pm 1$
	8 <sup>e)</sup>	La <sub>2</sub> O <sub>3</sub>	10–100	MMA	$6.35 \times 10^4$	1.23	0.48	$317 \pm 2$
	9	CeO <sub>2</sub>	10	MMA	$6.88 \times 10^4$	1.27	0.13	$244 \pm 1$
	10	WO <sub>3</sub>	60	MMA	$2.36 \times 10^5$	1.98	0.28	$762 \pm 5$
	Post-transition	11	$\alpha$ -Al <sub>2</sub> O <sub>3</sub>	30	MMA	$2.37 \times 10^5$	2.10	0.06
12		$\alpha$ -Al <sub>2</sub> O <sub>3</sub>	30	BA	$2.42 \times 10^4$	1.24	0.06	$385 \pm 1$
13		In <sub>2</sub> O <sub>3</sub>	20–70	MMA	$1.40 \times 10^5$	1.49	0.20	$377 \pm 9$
14		ITO	20–70	MMA	$1.23 \times 10^5$	1.92	0.11	$396 \pm 3$
15 <sup>e)</sup>		SnO <sub>2</sub>	35–55	MMA	$1.64 \times 10^5$	2.24	0.22	$377 \pm 1$
Metalloid	16	Sb <sub>2</sub> O <sub>3</sub>	80–200	MMA	$3.66 \times 10^5$	1.93	0.14	$870 \pm 20$
Metallate	17 <sup>f)</sup>	BTO	200	MMA	$1.85 \times 10$	2.38	0.43	$715 \pm 4$

a) Typical reaction conditions: [MO<sub>x</sub>-Br, assuming 1 Br nm<sup>-2</sup>]<sub>0</sub>/[M]<sub>0</sub>/[CuBr<sub>2</sub>]<sub>0</sub>/[Me<sub>6</sub>TREN]<sub>0</sub> = 1/1000/0.2/0.5, 50 vol% anisole, 1.0 mm × 1 cm copper wire, room temperature.

b) Determined by SEC.

c) Determined by molar mass and inorganic contents.

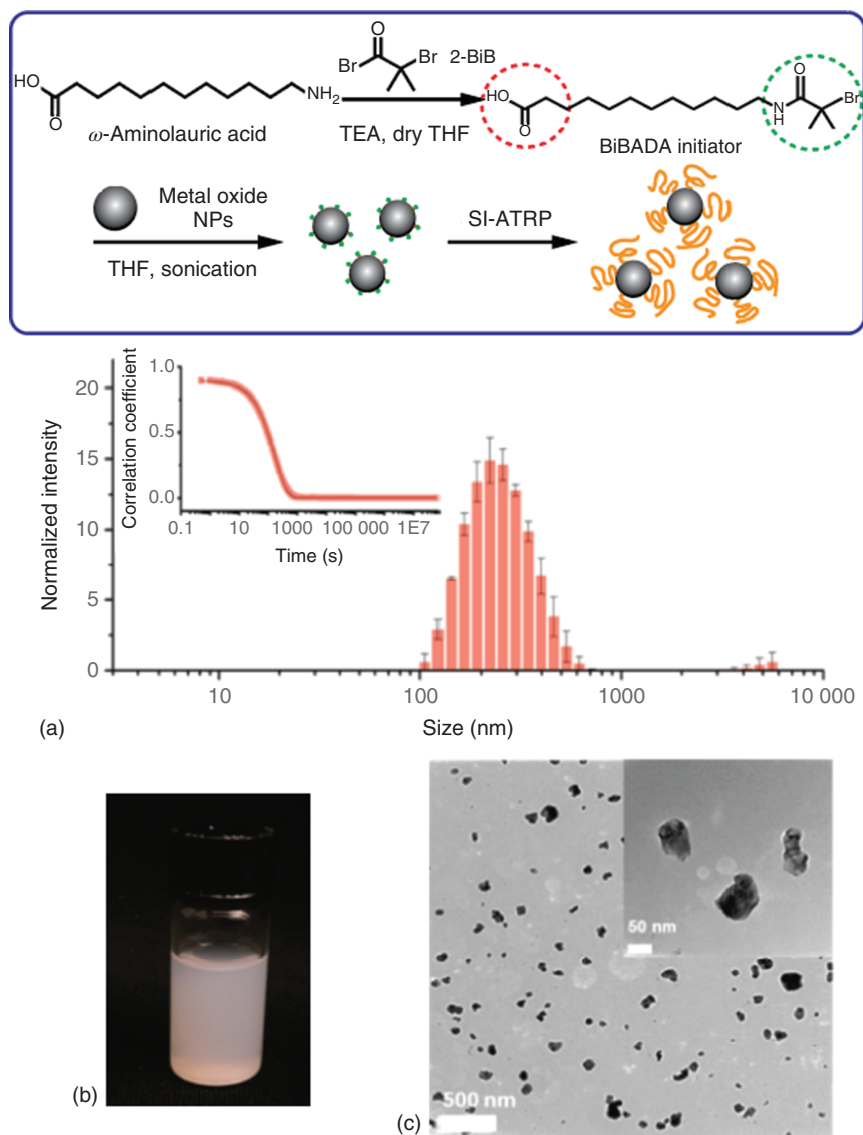
d) Z-Averaged hydrodynamic size in THF determined by DLS.

e) Nanoparticles functionalized with BiBADA.

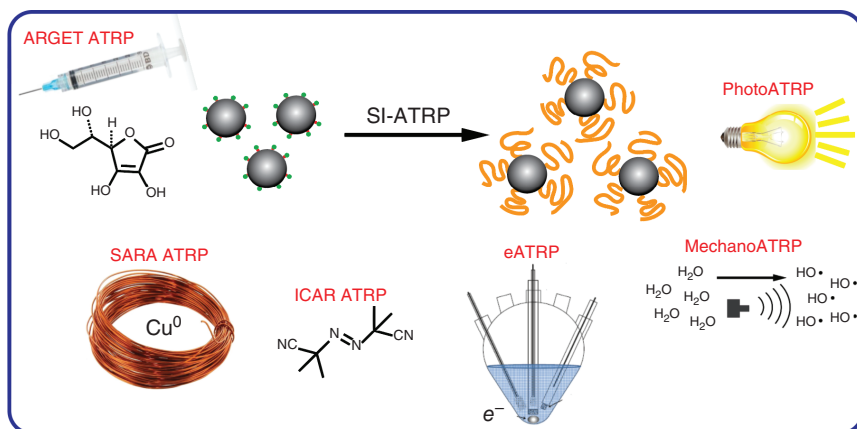
f) [BTO-Br, assuming 1 Br nm<sup>-2</sup>]<sub>0</sub>/[M]<sub>0</sub> = 1/3000.

Source: Reproduced with permission of Yan et al. [39], Copyright 2017, American Chemical Society.

but also allowed for spatial and/or temporal control over the process. Besides the Cu complex, other transition metal compounds, including Fe [144–146], Ru [147, 148], or Ir [149], could also regulate an ATRP equilibrium. The latest advancement of metal-free ATRP solved the dilemma of transition metal impurities in the polymer product. However, it is still challenging to reach a level of high versatility as well as good control over the reaction that is similar to Cu complexes [150–152]. The ATRP process was lately programmed by applying a DNA synthesizer, further expanding the versatility of this technique and promoting its efficiency [153]. Due to its potential to pattern the substrates with polymer ligands, ATRP procedures with external stimuli have drawn considerable attention to systems involving macroscopic substrates [154–159].



**Figure 1.2** Top scheme: synthesis of BiBADA and surface functionalization of metal oxide nanoparticles with polymer ligands. Characterization of ZrO<sub>2</sub>-g-PMMA nanoparticles: (a) Intensity-weighted hydrodynamic size distributions of ZrO<sub>2</sub>-g-PMMA as an example. (b) Photograph of a uniform dispersion of ZrO<sub>2</sub>-g-PMMA in THF. (c) TEM images of ZrO<sub>2</sub>-g-PMMA. Source: Yan et al. [39], Reproduced with permission of American Chemical Society.



**Figure 1.3** External control for various ATRP techniques. Source: Dmitry Kazitsyn/Adobe Stock.

The emergence of ARGET ATRP not only enabled the dramatic reduction of the concentration of copper complex catalyst to a ppm level but also facilitated the polymerization reaction to be tolerant to limited amounts of air [130, 131]. ARGET ATRP can be recognized as a “green” approach, which consumes ppm amount of the catalyst incorporated with the proper reducing agents including tin(II) 2-ethylhexanoate ( $\text{Sn}(\text{EH})_2$ ) [130], ascorbic acids [160], phenol [161], hydrazine and phenyl hydrazine [134], excess inexpensive ligands [162], amines, or nitrogen-containing monomers [163]. ARGET ATRP confirmed that SI-ATRP is readily applicable to large-scale manufacturing on macroscopic substrates [28, 157, 164], even under a certain level of oxygen exposure [165–169]. The repeated redox cycle between the transition metal complex and excess reducing agents consumed all oxygen in the reaction vessel [164]. Another important benefit of ARGET ATRP is that the transition metal complex triggered side reactions are significantly reduced [170]. This helps to further push an ATRP reaction to completion (full conversion) and synthesize copolymers with larger molar mass while preserving chain-end functionality [171, 172], which was confirmed by efficient chain extensions [173].

In ICAR ATRP, an addition of standard free radical initiators is employed to continuously regenerate the extremely low levels of Cu/L catalyst concentration (5–50 ppm). The use of initiators in the continuous activator regeneration procedure could be considered as a “reverse” ARGET ATRP. At this very low concentration of copper activator, in some applications, removing or recycling the transition metal catalyst residues is no longer necessary. The polymerization is promoted to high conversion with low concentrations of a source of organic free-radical initiators [134]. The polymerization rate in ICAR ATRP is determined by the rate of decomposition of the added initiator, while the rate of deactivation and the molecular weight distribution are governed by  $K_{\text{ATRP}}$  [174, 175].

$\text{Cu}^0$  wire ( $\text{Cu}^0$ ) can act as a reducing agent and induce a  $\text{Cu}^{\text{II}}$  deactivator disproportionation to produce the  $\text{Cu}^{\text{I}}$  species [176].  $\text{Cu}^0$  can also play the role of a

supplemental activator, where it directly reacts with alkyl halides and generates a propagating radical, even though a majority of the activation of alkyl halides is triggered by the  $\text{Cu}^{\text{I}}$  activator. Hence, this procedure is known as SARA ATRP [177]. The use of other transition metals, such as metallic Zn, Mg, Fe, and Ag, was explored to lower the deactivator concentration in ATRP [177, 178].

The use of chemical reducing agents generated oxidized residues in the polymer product. Therefore, it is important to develop a procedure of reduction via nonchemical means. Electrochemical reductions provide various easily tunable parameters to tune polymerization rates by pursuing the preferred concentration of the redox-active transition metal complexes. For example, a desired percentage of the  $\text{Cu}^{\text{II}}\text{Br}_2/\text{Me}_6\text{TREN}$  deactivator species can be electrochemically reduced to  $\text{Cu}^{\text{I}}\text{Br}/\text{Me}_6\text{TREN}$  activators to initiate a controlled ATRP reaction. The employed potential determines the activator/deactivator ratio ( $[\text{Cu}^{\text{I}}/\text{L}]:[\text{Cu}^{\text{II}}/\text{L}]$ ), thus the rate of polymerization [136]. Temporal control of the reaction has become particularly valuable in SI-ATRP, as it offers the possibility to “pause/restart” the polymerization to check and monitor the status of reactions [179]. This procedure also enables temporal control over the polymerization, simply by switching on/off the current. The molar mass of polymer chains formed in the *e*ATRP process grew linearly with monomer conversion and a low dispersity was achieved. The concentration of catalytic complex as low as 50 ppm was sufficient to retain a controlled polymerization showing first-order kinetics and narrow molecular weight distribution. Cu can be electrodeposited on the electrode and stripped, affording efficient catalytic complex regeneration [180]. *e*ATRP was also employed to synthesize gradient copolymer grafted hairy nanoparticles where the thickness of polymer shell was governed by tuning space/location of the supporting substrates from the electrode [158, 181].

Due to the simple set-up, insignificant usage of additives, and a possible choice of employing daylight, the PhotoATRP procedure attracted considerable attention [138, 156, 182–190]. PhotoATRP was expanded from copper to iron as the metal catalytic complex [146]. PhotoATRP was successfully performed with ppm amounts of copper catalysts [183, 184, 191]. PhotoATRP in either organic solvents or aqueous solutions was carried out. Precise and well-defined control over polymerization in PhotoATRP enabled efficient chain extension as well as the preparation of block copolymers. The polymerization can be paused and restarted simply by switching on/off the photo-irradiation source. The excited copper catalytic complexes ( $\text{Cu}^{\text{II}}/\text{L}$ ) were reduced in the presence of electron donors [182]. PhotoATRP from inorganic substrates was later extended to SI-PhotoATRP facilitated by an organic photoredox catalytic complex, generating precisely controlled polymer hybrid nanocomposites without metal residues [33, 179, 192].

The metal-free ATRP was mediated by photo-irradiation with multiple organic photoredox catalysts, including phenothiazines, phenazines, and phenoxazines [150, 152, 193, 194]. The metal-free ATRP showed excellent versatility for a broad range of different methacrylate monomers. Successful chain extension and block copolymer synthesis were combined with other CRP procedures, resulting in synthetic and morphological versatility. Furthermore, phenothiazine derivatives were utilized as novel metal-free photoredox catalytic complexes for the PhotoATRP



of polyacrylonitrile (PAN) with desired molar mass and narrow molecular weight distribution. The well-preserved halogen chain-end fidelity of the synthesized PAN was confirmed either by the  $^1\text{H}$  NMR spectrum or the successful chain extension reaction [151].

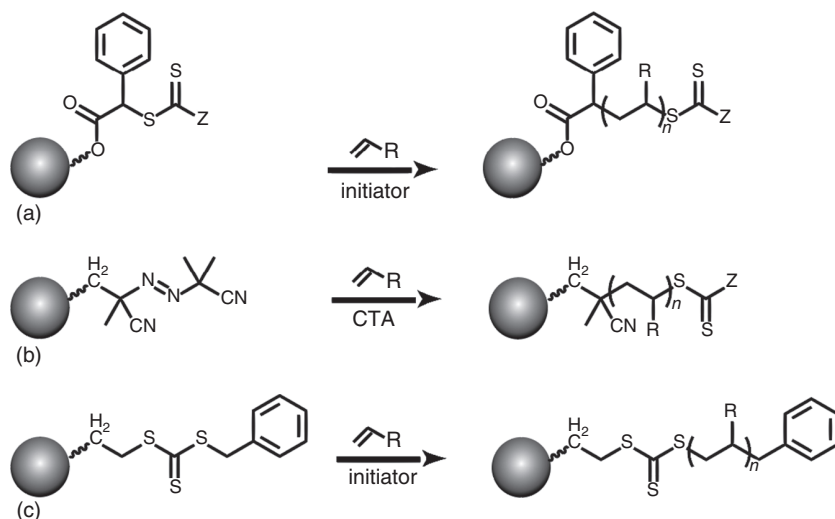
A robust mechanically controlled ATRP of methyl acrylate was performed in an ultrasound bath with a ppm level concentration of copper catalyst by means of ultrasonication as the external stimulus and piezoelectric nanoparticles  $\text{BaTiO}_3$  (barium titanate) as the mechano-electrical transducing materials in DMSO solution, using a frequency of 40 kHz [141, 195]. It was recently demonstrated that zinc oxide nanoparticles ( $\text{ZnO}$ ) are even more efficient than  $\text{BaTiO}_3$  as piezoelectric material and could be applied in c. 100 times lower amount than  $\text{BaTiO}_3$  [140].

### 1.3.1.3 SI-RAFT

RAFT polymerization is another well-explored CRP technique. The dynamic exchange in a RAFT process is based on the reversible addition-fragmentation of initiating/propagating radicals to chain transfer agents (CTAs), including dithioester or trithiocarbonate, Figure 1.1 [196, 197]. The most important characteristic of RAFT polymerization is that it is mainly based on the classic FRP setups with the added RAFT agents. Free radical initiating species are applied to form the propagating species and maintain the polymerization rate; meanwhile, the concentration of RAFT agents defines the targeted molecular weight. RAFT polymerization involves degenerative chain transfer, which assures all the polymer chains propagate at the same rate, leading to polymers with narrow molecular weight distribution [198]. Compared to ATRP, the RAFT process can be used to polymerize some less reactive or functional monomers [199]. In addition, the colored reactive RAFT chain ends are usually needed to be removed to purify the harmful residues from the polymer product [200]. Moreover, external stimuli were also employed in RAFT polymerizations, such as photoinduced electron/energy transfer (PET)-RAFT polymerization [186, 201]. Unlike the classic RAFT polymerization, the propagating species in PET-RAFT is formed by the PET-excited photoredox catalytic complex from the RAFT agent. Thus, as the process does not require any free radical initiators, it exhibited a superior oxygen tolerance and excellent temporal/spatial control performance [186]. Other external controls, including ultrasound agitation [202] and electrochemical method [203], were also thoroughly investigated for the RAFT polymerization. Occasionally, oxygen can act as an external trigger for RAFT polymerization [204].

SI-RAFT polymerizations were also exploited [205]. The first reported SI-RAFT reaction was accomplished via the mechanistic transformation of an SI-ATRP polymerization [206]. An alternative approach to carry out a RAFT reaction was to trigger the reaction from tethered azo initiators on the surface and control the polymerization through free RAFT agents in the dispersion [207]. Polymerizations were also performed by directly immobilizing CTAs on the surface with initiating species in the reaction mixture [51].

SI-RAFT polymerization could be performed either via surface-tethered free radical initiating sites or surface-functionalized RAFT CTA agents. Generally, there



**Figure 1.4** Three main approaches to surface RAFT polymerization: (a) Using a R-Group Anchored CTA, (b) Using a Surface Immobilized Initiator, and (c) Using a Z-Group Anchored CTA.

are three different ways to carry out SI-RAFT polymerization from the surfaces, based on how the CTA is immobilized, Figure 1.4. With free radical initiating sites immobilized on the surface and untethered CTAs in solution, SI-RAFT exhibited the same kinetic features as SI-FRP [207]. In other approaches, either the R-group [206, 208] or the Z-group [209, 210] of the CTA was attached to the surface, a process termed SI-RAFT polymerization as the initiation step occurs in the reaction solution [4]. In the R-group anchoring case, the anchored CTA is typically synthesized from an ATRP initiator or its derivatives [208, 211]. The broad range of various functional CTAs, for instance, 4-(4-cyanopentanoic acid) dithiobenzoate, affords an alternative option for immobilizing the CTA functionalities in a direct/indirect manner [212]. The SI-RAFT polymerization performs similarly to SI-ATRP; however, as the system contains the same number of growing radical chain ends and untethered CTAs, the deactivation process is typically less efficient, resulting in broader molecular weight distribution. Furthermore, SI-RAFT polymerization applying Z-group anchored CTA encountered the same dilemma as the “grafting-onto” method, as the tethered CTA on the surface progressively became inaccessible to the active chain ends. Despite the anchoring method applied, untethered free polymers are generally unavoidable in SI-RAFT polymerization. Nevertheless, SI-RAFT polymerization has some advantages, especially the ability to polymerize functional monomers or monomers with low reactivities [213]. Recently, PET-RAFT from surfaces was also reported [214, 215].

One approach to carry out SI-RAFT polymerization is to immobilize an azo initiator to the surface and perform the reaction in the solution containing untethered CTAs. This method has been employed to polymerize a range of monomers, such as (vinylbenzyl)trimethylammonium chloride [216], glucose-based monomers

[217], methacrylate [218], benzyl methacrylate [219], 2-(dimethylamino)ethyl methacrylate [218], *N*-isopropylacrylamine [219–221], *N*-acetylmuramic acid [221], styrene [222], acrylic acids [223, 224], and acrylamide [224]. A more conventional method to perform SI-RAFT polymerization is to immobilize the CTA onto the surface and add the radical initiating species in the solution. This method has been employed to generate polymer chains from multiple substrates, including carbon nanotubes [225, 226], quantum dots [227], gold surfaces [228–230], iron oxide nanoparticles [37, 211, 231–234], graphene [235], SiO<sub>2</sub> nanoparticles [211, 236–253], BaTiO<sub>3</sub> [254], ZnO/ZnS [255], and TiO<sub>2</sub> nanoparticles [256]. Although there are two options to immobilize the RAFT agents in the solution-initiated SI-RAFT polymerization, either through the reinitiating R-group of the CTAs or the stable Z-group, there is a preference for tethering the RAFT agent through the R-group.

There are mainly two approaches to functionalize surfaces with RAFT agents. In the first method, the CTA is prepared with an active functional moiety that can be covalently linked to the pristine surface. The second method is based on attaching the CTA to a pre-functionalized substrate to preserve anchoring moieties, corresponding to the functionality of the RAFT agent. The first approach generally is more challenging, but it has been employed for a broad range of substrates. The other approach has its benefits, as it simplified the purification step for the RAFT agents and helped to diminish some general secondary reactions, for instance, the condensation of CTA-bound alkoxy silane groups. Under the same principle, click chemistry was employed to tether CTAs to SiO<sub>2</sub> nanoparticles [257]. Additionally, halide functionalized substrate surfaces can be applied to anchor suitable reactive RAFT agents and their derivatives. Last but not least, pre-synthesized RAFT agents can also be attached to electroconductive substrates through the electrochemical method, such as gold [228, 229].

#### 1.3.1.4 Other Polymerization Techniques

In addition to SI-ATRP and SI-RAFT, other controlled polymerization approaches, such as SI-NMP, living anionic polymerization (LAP), living cationic polymerization (LCP), and ring-opening metathesis polymerization (ROMP), are practical techniques to prepare hair nanoparticles.

NMP was one of the first-reported RDRP methods [258]. In this approach, the dormant species (for example, alkoxyamine) involves homolysis of the carbon–oxygen covalent bond at relatively high temperatures to generate an active propagating radical and a persistent nitroxide species [259–264], Figure 1.1. Later, SI-NMP was reported as another approach to graft polymer chains from the substrates. Only monomers and alkoxyamine-functionalized substrates are required for this technique. Alkoxyamine-functionalized surfaces can be synthesized either via modification of anchoring alkoxyamine [265–267] or by reacting reactive surface radicals with nitroxide radical species [268, 269]. However, SI-NMP presents the limitations of NMP, as it shows the difficulty to polymerize non-styrenic monomers, especially acrylic and methacrylic monomers. Recently developed anchoring derivatives of alkoxyamines with high activity were used in SI-NMP,

accomplishing higher efficiency and allowing the polymerization of challenging acrylic monomers [266, 268–270].

In addition to radical polymerizations, ionic polymerizations have been demonstrated as feasible techniques for grafting polymer brushes from surfaces. Both LCP and LAP have a longer history than RDRP [271–273]. Living ionic polymerization was discovered earlier because the ionic intermediates do not undergo bimolecular termination as in radical polymerization. However, cationic polymerization is typically less “living” than anionic polymerization because of proton transfer to monomer reactions, which leads to termination/chain transfer.

Surface-initiated ionic polymerizations are far less studied than SI-RDRP because of the highly reactive carbocation or carbanion intermediates, requiring extremely delicate experimental setups, especially for nanoparticles with high surface areas. In addition, ionic polymerizations are compatible with a narrower selection of monomers than radical polymerization. Nonetheless, ionic polymerizations are employable to monomers that do not undergo radical homopolymerization.

To introduce carbanion to a surface, a similar technique as homogeneous anionic polymerization was used, i.e. the reaction between immobilized 1,1-diphenylethylene and butyl lithium [274]. Carbocation, on the other hand, was introduced in two different ways. It can be generated by Lewis acid-induced cleavage of immobilized ether [275]. Otherwise, in a way similar to surface RAFT polymerization with Z-group-anchored CTAs, surface-initiated cationic polymerization can be initiated by reacting the surface silanol group of silica with p-methoxybenzyl alcohol in the presence of sulfuric acid to generate p-methoxybenzylum cations stabilized by surface adsorbed hydrogen sulfate anions, and therefore proceed with the polymerization with the nanoparticle as a “macro-counterion” [276].

Ring-opening polymerization (ROP) is capable of polymerizing a specific class of cyclic monomers. Therefore, many hairy nanoparticles inaccessible from the polymerization of vinyl polymers can be prepared via SI-ROP. Although the same carbanion or carbocation initiators used for ionic polymerization can also initiate ROP, less reactive initiators are often used because of the easier experimental handling. For example, in anionic ROP, weaker bases such as alkoxides or amines may initiate the polymerization of a wide range of cyclic monomers, such as caprolactone, lactide, or *N*-carboxyanhydride [277–282]. Polymerization of *N*-carboxyanhydride is especially intriguing because it yields peptide brushes [277]. Similarly, cationic ROP can be initiated with alkylation agents such as tosylates. Biocompatible poly(2-oxazoline)-based hairy nanoparticles were prepared this way [283, 284].

ROMP polymerizes cyclic olefin monomers with metallic carbene species as initiators [285–288]. With the rational design of the catalyst, such as Grubbs catalyst third generation, ROMP exhibits excellent control of polymerization and good tolerance to the ambient atmosphere, impurities, and monomer functionalities [289, 290]. Typical ROMP monomers include cyclooctene, norbornene, macrocyclic olefins, and their derivatives [291, 292]. Norbornene derivatives allow an especially rich variety of functionalities, comparable to acrylic monomers of radical polymerization. To initiate ROMP from a surface, a cyclic olefin has to be first immobilized, and a one-step olefin metathesis transfers the metallic carbene to the surface [293, 294]. Subsequently, ROMP can be performed using these immobilized metallic carbenes

as initiators. Several intrinsic challenges limit the broad application of SI-ROMP in the preparation of hairy nanoparticles. Both ROMP monomers and catalysts, such as ruthenium, tungsten, and molybdenum complexes, are more expensive than those for RDRP. Such metallic catalysts/initiators in ROMP, become unfavorable impurities in the final product. While ATRP can be performed with a ppm catalyst loading, ROMP requires one metal atom per chain, resulting in higher costs and more metallic residues. Although metal-free ROMP was recently reported, there are still many challenges and no application for surface-initiated systems [295]. Another issue with ROMP is backbiting [286]. As the reactive carbon-carbon double bonds are also present in the polymer backbone, active chain-end attacks on the backbone can lead to undesired loops, free polymers, and/or broadened molecular weight distribution in the preparation of hairy nanoparticles. This also limits the available choice of monomers and catalysts for SI-ROMP when backbiting must be inhibited.

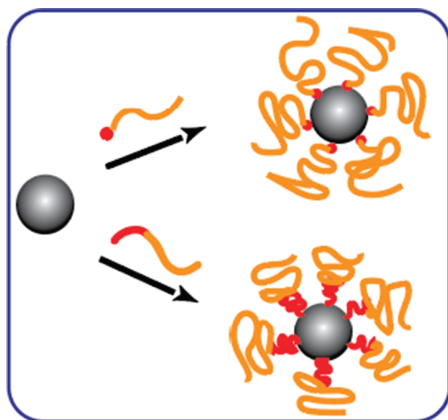
### 1.3.2 The “Grafting-onto” Approach

Compared to the “grafting-from” approach, the “grafting-onto” approach is generally recognized as a more simple technique. Minimal surface modification is needed as a suitable anchoring functionality can usually be exposed for the pristine surface functional groups. However, due to the strong steric hindrance among the already-grafted polymer chains, it is challenging to obtain high grafting densities through the “grafting-onto” approach [296]. Typically, a more diluted graft layer with a grafting density well below 1.0 chains  $\text{nm}^{-2}$  was typically obtained through the “grafting-onto” approach, which resulted in a collapsed mushroom-like topology [297].

#### 1.3.2.1 Conventional “Grafting-onto” Approach

Polymer chains can be attached to inorganic substrates when one functional chain end/block is reactive, which can promote connection to the substrate. Generally, such anchoring groups can be the functional end groups of polymer ligands [113, 298], comonomers incorporated through copolymerization or a chain-end functionality tethered by transfer agents [299]. Nevertheless, reacting the active functional end groups through the polymerization requires strict conditions. In the case of copolymer synthesis, when the comonomers are added along with the polymerization, a governing of the sequence of the functional comonomers in the backbone is needed to diminish the generation of unrestrained loop structure on the surface. On the other hand, polymers like poly(ethylene oxide), poly(propylene oxide), and poly(dimethylsiloxane) have intrinsic functional chain ends, which could be directly applied for anchoring [300, 301]. Despite its advantages, this approach is only applicable to a limited range of polymers, as many of them are multifunctional and can lead to the formation of a mixture of hairy nanoparticles and loops. Moreover, the gelation by interparticle coupling could likely occur during the procedure of grafting-onto (Scheme 1.5).

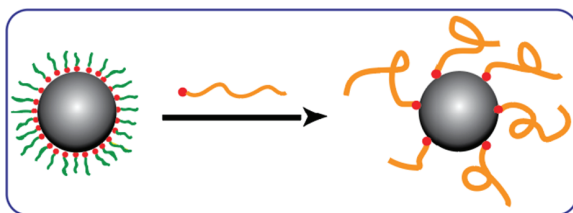
CRP allows precise control over the grafting performance of the polymer ligands on the surface and enables the synthesis of polymers with well-tuned chain length, composition, chain-end fidelity, and chain architectures. For instance, in RAFT polymerization, the sulfur-terminated end group is suitable to be used to



**Scheme 1.5** The “grafting-onto” approach.

graft polymer ligands onto noble metal surfaces. Another example was adding sodium borohydride to reduce the dithioester functionality of the thiol group, tethering gold nanoparticles [302, 303]. Polymerizations initiated by functional RAFT agents yield functional group-terminated polymer ligands used in the “grafting-onto” approach. For instance, esterification of propargyl alcohol with 4-cyanopentanoic acid dithiobenzoate produces an alkyne-terminated CTA, resulting in alkyne-terminated polymers. The chains can further be attached to a surface through a copper-catalyzed azide-alkyne cycloaddition (CuAAC) process [304]. A similar process has been applied to the ATRP procedure as well [104]. Meanwhile, as the same copper catalytic complex is involved among all CuAAC, ATRP, and Glaser coupling steps, some secondary side reactions could occur [305]. Another approach is to prepare azide-terminated functional groups by halogen substitution of the chain-end functionality with an azide [306–308]. Additional end functional groups, including phosphonate and thiol, for selectively applying to iron oxide and gold substrates, can be incorporated into polymers through ATRP reaction from pre-functionalized initiators as well [43, 309, 310]. Moreover, Y-shaped polymer ligands grafted substrates were prepared when the functional groups were introduced in the middle of the backbone instead of the chain ends [311].

An alternative option for the “grafting-onto” approach is to use functional block copolymers containing blocks with distinct surface affinities. Normally, just a weak attraction between the anchoring block with surface affinity and the target surface is enough to link the block copolymer ligands to the substrate, the non-tetherable block functions as the polymer “free” chain. If there are multiple anchoring groups present in the block copolymers, the formation of a loop structure can be achieved by the non-affinity segments between the anchoring functionalities [312]. In the diblock copolymers, the blocks without anchoring groups, instead of always fully collapsing, tend to form a partially stretched conformation, as the chain grows [313]. Grafting block copolymers with different anchoring abilities onto surfaces can be applied to disperse and compatibilized inorganic nanofillers



**Scheme 1.6** The “ligand exchange” approach.

in different media, including aqueous/organic solutions, or polymer matrices [103, 314, 315]. The different affinities between the two blocks were essential to avoid the agglomeration of nanofillers. For instance, compared to poly(acrylic acid)-*block*-poly(styrene-*co*-acrylonitrile) (PAA-*b*-PSAN) ligands, PAA-*b*-PMMA ligands give better performance as the dispersant for separating ZnO nanoparticles in organic solutions, as the higher polarity acrylonitrile segments might compete with the PAA blocks and cause coupling of ZnO nanoparticles [103]. Besides, amphiphilic triblock copolymers poly(methacrylic acid)-*block*-poly(methyl methacrylate)-*block*-poly(styrene sulfonate) (PMAA-*b*-PMMA-*b*-PSS) were adsorbed to the surfaces of Fe<sup>0</sup>/Fe<sub>3</sub>O<sub>4</sub> nanoparticles as physisorbed layers to improve the dispersion stability of the nano-iron suspensions in aqueous system and facilitate their adsorption at the water/oil interface [316–318].

### 1.3.2.2 Ligand Exchange

The “ligand exchange” approach involves the substitution of the small-molecule ligands on the surface of the inorganic substrates with different functionalized polymer ligands, which is a special case of the “grafting-onto” approach. To fulfill the ligand exchange’s prerequisite conditions, either the polymer ligands present a stronger affinity to the inorganic surface than the pristine ligands or the small-molecule ligands can be removed from the system during the reaction to promote the ligand substitution process (Scheme 1.6).

The first-reported ligand substitution reaction was carried out between the pristine phosphine oxide ligands and the poly(2-(dimethylamino)ethyl methacrylate) (PDMAEMA) ligands on the CdSe/ZnS quantum dots. In the organic medium, the replacement from labile small-molecule ligands to bulky polymer ligands gave stable and uniform coverage over the quantum dots [319]. However, the polymer-stabilized quantum dots synthesized through this technique exhibited some significant limitations, as the reaction strongly relied on the dynamic equilibrium between the two ligands. The polymer ligands containing carbodithioate functional groups can easily replace the pristine trioctylphosphine oxide ligands due to their substantially larger affinity to the surfaces of CdSe/ZnS quantum dots [320]. In a similar manner, a monofunctional thiol group is generally efficient enough to substitute less stable ligands on noble metal substrates [321].

The surface affinity or the reactivity of the anchoring chain-end groups in polymer ligands will significantly decrease as the chain grows, resulting in an incomplete ligand exchange reaction even with an excessive addition of the desired ligands [322].

This can be resolved in an improved method by using a non-solvent for the small ligands stabilizing nanocrystals as well as the polymer ligands. The precipitation of the nanocrystals with polymer ligands as aggregates from the solutions can locally exclude the fully soluble small pristine ligands and increase the concentration of polymer ligands, the polymer-capped nanocrystals are non-dispersible in the solvent, driving the equilibrium of the ligand exchange reaction further forward to completion.

Compared to the conventional “grafting-onto” approach, a high grafting density can be afforded by the ligand exchange method through gradual substitution of the densely capped nanoparticles with polymer ligands, and a grafting density of up to 1.2 chains  $\text{nm}^{-2}$  was achieved. For a ZnO-based hairy nanoparticles synthesis, a relatively low boiling point (175 °C) ligand – octylamine was selected as the removable pristine ligands [38]. By heating the reaction mixture above the boiling point of octylamine, the volatile ligands were continuously removed from the system, thus shifting the equilibrium of the ligand exchange process. With the addition of  $\text{NH}_2$ -terminated PSAN ligand, PSAN- $\text{NH}_2$ , which was synthesized through ARGET ATRP, the obtained PSAN-capped ZnO nanoparticles were used as high-refractive index nanofillers in transparent acrylic glasses [323], as well as the precursors of carbon-ZnO hybrids for photocatalytic and electrochemical applications [324, 325]. The achieved grafting density of PSAN-capped nanoparticles through this approach was 0.9–2.5 chains  $\text{nm}^{-2}$ , depending on the ratio between ZnO nanoparticles and the desired polymer ligands.

### 1.3.3 Template Synthesis

The “grafting-from” and “grafting-onto” modifications discussed above can be considered as “inorganic-first” approaches. On the other hand, the synthesis of hairy nanoparticles through polymeric templates can be categorized as a “polymer-first” approach. In this approach, inorganic fillers are produced within the inner template, and the remaining outer polymeric shells serve to stabilize the nano-objects. The molar mass, molecular weight distribution, chain composition, and architecture of the pre-synthesized polymer templates can be well-tuned to achieve complex morphologies, which can be also encoded in the hairy nanoparticles.

#### 1.3.3.1 Block Copolymer and Its Derivative Templates

Linear polystyrene (PS)-based block copolymer templates, such as polystyrene-*b*-poly(2-vinyl pyridine) (PS-*b*-P2VP), polystyrene-*b*-poly(ethylene oxide) (PS-*b*-PEO), or polystyrene-*b*-poly(acrylic acid) (PS-*b*-PAA) templates, loaded with different metallic precursors were fabricated into metal or metal oxide nanoparticles/polymer nanocomposite films through reduction reactions [105, 326–328]. Surfactants can prevent aggregation, define the size, and shape of the nanoparticles, as well as their compatibilization with the medium, thus playing a critical role in inorganic nanoparticle preparation [329]. In the presence of surfactants as templates, the precursors in the micelles transform into inorganic nanofillers. Instead of the conventional organic surfactants, the block



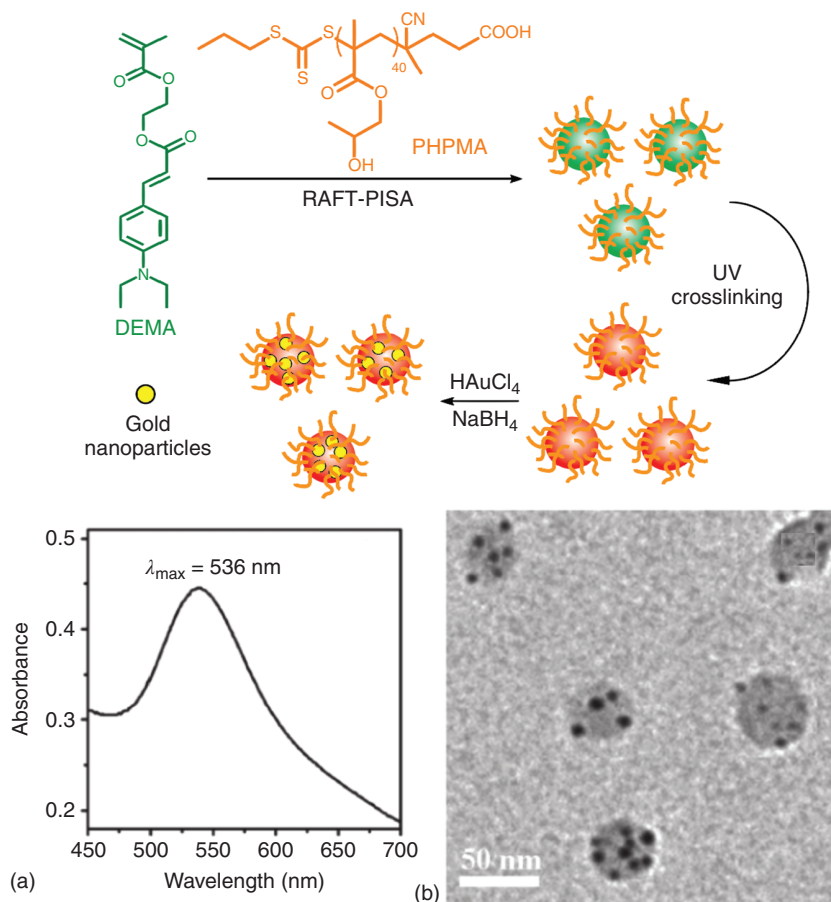
copolymer micelles were reported as a liquid-phase template [105, 326, 330]. The poly(methyl methacrylate)-*b*-poly(ethylene adipate)-*b*-polyvinylpyrrolidone (PMMA-*b*-PEA-*b*-PVP) random copolymers were used to govern the decomposition of  $\text{Co}_2(\text{CO})_8$  and induce the formation of well-defined Co nanoparticles [331, 332]. The initial templated approach focused on the use of block copolymers to facilitate the formation of micelles in solution, providing limited rational design beyond the formulation adjustments [333, 334]. The amphiphilic nature of the block copolymers endorses the use of water/oil emulsions. Inorganic/polymer hybrids were synthesized when the inorganic fillers were formed inside the emulsion droplets. On the other hand, porous inorganic materials were generated when the continuous phase was made of inorganic precursors. Later, the polymeric template-assisted synthesis of metal/metal oxide nanoparticles [333, 335–339] was further investigated with polystyrene-*b*-poly(4-vinyl pyridine) (PS-*b*-P4VP) or PS-*b*-P2VP as copolymer templates. Au [336, 338–340], Pd [336, 341], Pt [336], Rh, Co, and CdS [337] colloidal nanoparticles were synthesized from  $\text{HAuCl}_4$ ,  $\text{Pd}(\text{OAc})_2/\text{Na}_2\text{PdCl}_4$ ,  $\text{K}[\text{Pt}(\text{C}_2\text{H}_4)\text{Cl}_3]\cdot\text{H}_2\text{O}$ ,  $[\text{Rh}(\text{CO})_2\text{Cl}]_2$ ,  $\text{Co}_2(\text{CO})_8/\text{CoCl}_2$ , and  $\text{Cd}(\text{OAc})_2$ , respectively. The catalytic efficiency [338], and magnetic and optical properties of the obtained hybrid nanocomposites were characterized [337, 341]. Moreover, the recent development of polymerization-induced self-assembly (PISA) furthermore facilitated template-assisted synthesis by enabling more complex morphological control, such as the worm-to-vesicle transitions [342–346]. Such a control using PISA templates can allow the synthesis of inorganic nanoparticles of various sizes and shapes [106, 347]. For example, photo-crosslinkable and amine-modified poly(2-hydroxypropyl methacrylate)-poly(2-((3-(4-(diethylamino)phenyl)acryloyl)oxy)ethyl methacrylate) (PHPMA-PDEMA) block copolymer nanoparticles were synthesized via RAFT-PISA, and the crosslinked nanoparticles were applied as templates for polymer/gold hybrid nanoparticles (Figure 1.5) [348].

### 1.3.3.2 Star/Bottlebrush Polymer Templates

Star and bottlebrush block copolymers can be generally recognized as stable unimolecular templates. Recent publications introduced a universal synthetic route for the preparation of polymer-inorganic hybrid nanoparticles/nanorods using star/bottlebrush polymers with block copolymer arms as nanoreactors Scheme 1.7 [103, 110, 350]. The detailed discussion of the "polymer template approach" is covered in Chapter 3.

## 1.4 The Role of "Architecture" in Hairy Nanoparticles

The grafted polymer chains on the surface of nanoparticles are generally used to stabilize nanofiller dispersion within the polymeric host matrix and therefore play a critical role in the binary hybrid nanocomposites. Recent advances in hairy nanoparticles synthesis inspired various novel applications in the fields of gas separation [351–354], lubrication [355–361], antifouling [47, 312, 362–364],

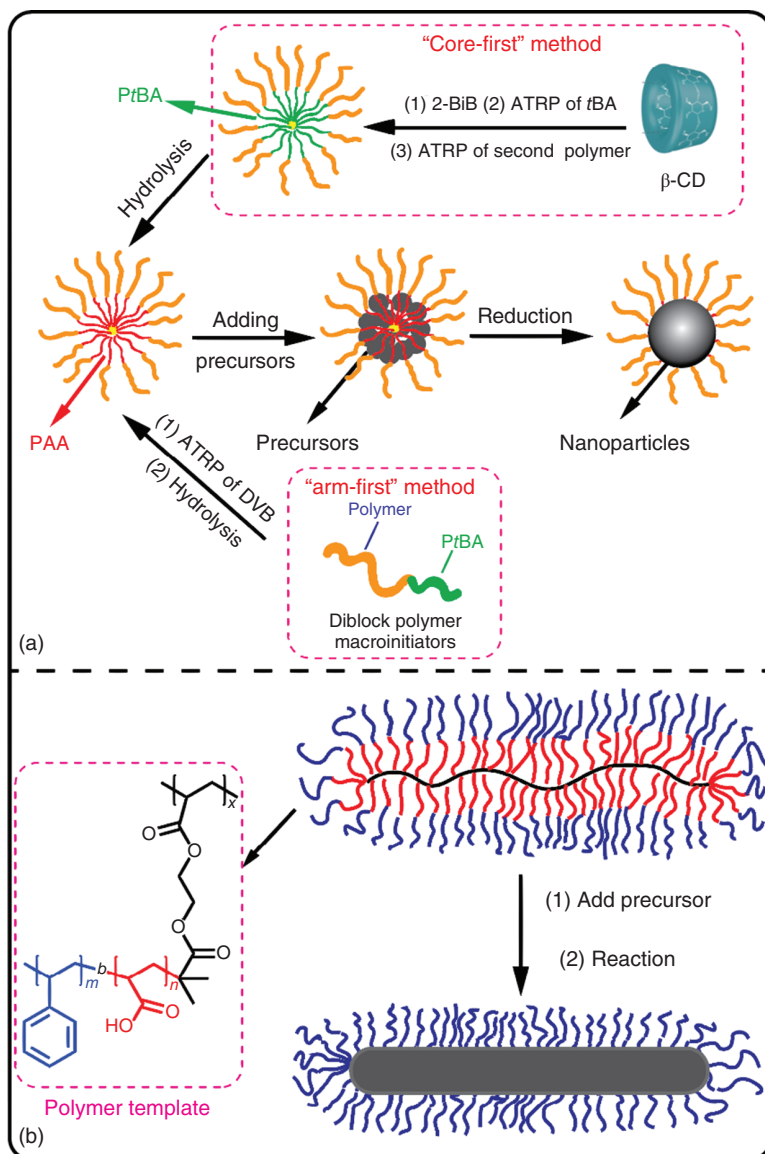


**Figure 1.5** Reaction scheme for the synthesis of photo-crosslinked stable PHPMA–PDEMA nanoparticles and preparation of gold/polymer nanoparticle composite. (a) The spectrum of solution after reduction of chloroauric acid using  $\text{NaBH}_4$ , (b) TEM image of the gold/polymer hybrid nanoparticles (molar feed ratio of  $\text{HAuCl}_4$ /tertiary amine is 1/4). Source: (b) Huang et al. [348], Reproduced with permission of John Wiley & Sons Inc.

smart-responsive materials [365–370], so on and so forth, Scheme 1.8. The properties of hairy nanoparticles are strongly associated with the chain architecture as well as the molecular characteristics of the tethered polymer ligands. The advances in synthetic methods to precisely modulate the architecture of polymer ligands, hence give a valuable research opportunity in the field. Major tools of macromolecular engineering include molar mass, dispersity, ligand composition, topology, and functionality. They also include multiple types of copolymers as well as bimodal ligands, miktoarm (binary) ligands that can be separated and assembled into Janus particles.

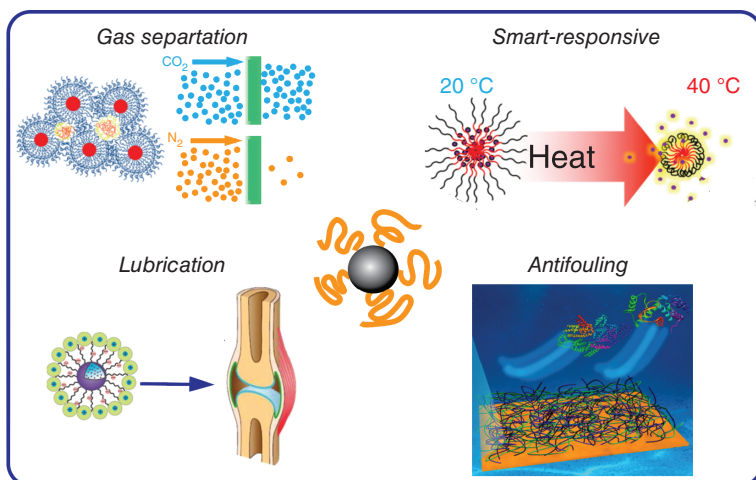
#### 1.4.1 Conformation of Hairy Nanoparticles

It is important to study the structure of hairy nanoparticles as it affects the physicochemical properties of hairy nanoparticles both in solid and solution states. The



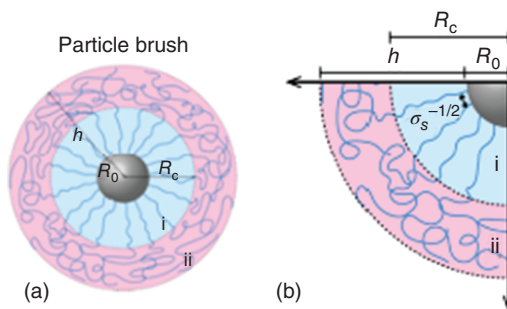
**Scheme 1.7** Synthesis of hairy nanoparticles/nanorods through (a) star polymer templates, (b) bottlebrush polymer templates. Source: Reproduced from Wang et al. [349] with permission of American Chemical Society, Copyright 2021.

main features of both the dynamic performance and interactions in hairy nanoparticles can be described using a scaling model that was first established by Daoud and Cotton (DC) to evaluate the structure of star-like polymers, which were later extended to hairy nanoparticle systems [371, 372]. According to the DC model, the structure of hairy nanoparticles can be divided into two regimes: the concentrated particle brush (CPB) regime and the semi-dilute particle brush (SDPB) regime.

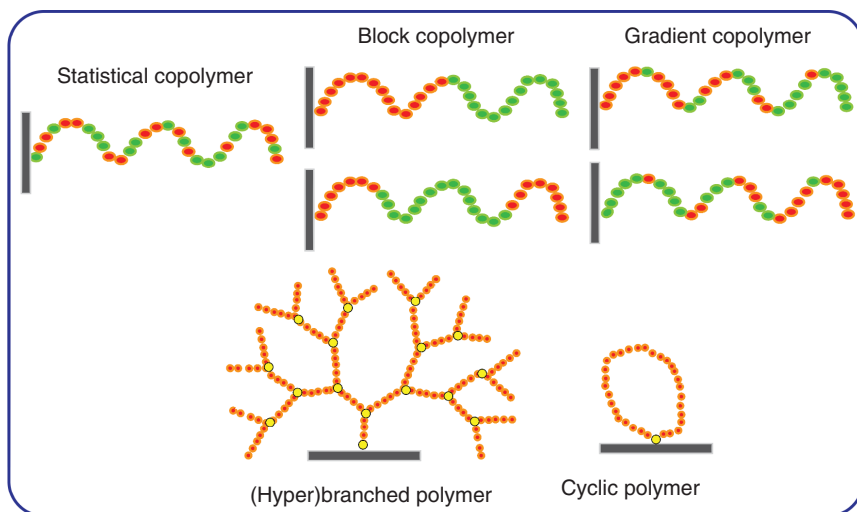


**Scheme 1.8** Schematic representation of the advanced application of hairy nanoparticles. Source: Adapted from Refs. [352, 355, 362, 369].

Within the CPB regime, due to the strong excluded volume interactions, chains maintain a stretched conformation, while in the SDPB regime, polymer chains preserve a relaxed mushroom-like conformation (Figure 1.6a). The critical distance  $r_c = r_0(\sigma^*)^{1/2}(\nu^*)^{-1}$  (where  $r_0$  refers to the particle radius,  $\sigma^* = \sigma a^2$  is the reduced grafting density,  $a$  is the length of a repeat unit, and  $\nu^* = \nu/(4\pi)^{1/2}$  is the effectively excluded volume parameter) [371] is given to defining the transition threshold between the two regimes: for a total effective hairy nanoparticles size  $r_0 + h < r_c$  (where  $h$  refers to the thickness of the polymer shell), they are presumed to be in the CPB regime. On the other hand, for a total effective hairy nanoparticle size  $r_0 + h > r_c$ , the SDPB regime is expected (Figure 1.6b). In the ideal scaling model, in the CPB regime, the thickness of the polymer shell scales  $h \sim N^x$  ( $1 > x > 3/5$ ),



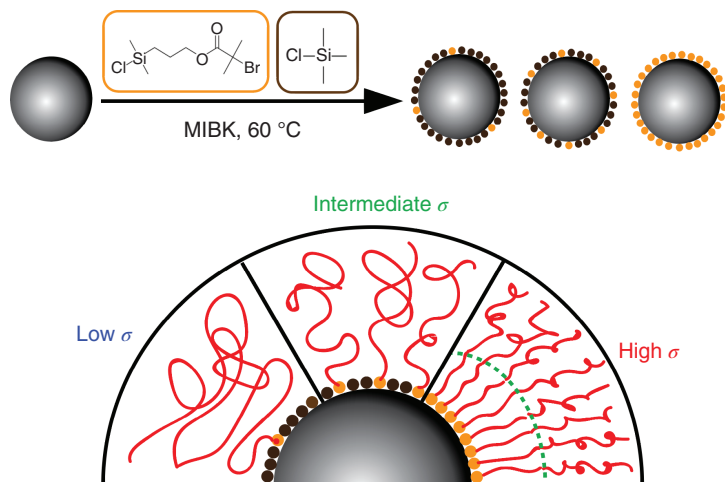
**Figure 1.6** Illustration of the transition from concentrated particle brush to semi-dilute particle brush regime. (a) A hairy nanoparticle with radius  $R_0$  and grafting density  $\sigma_s$  shows the concentrated particle brush and semi-dilute particle brush regimes with stretched and relaxed chain conformations. (b) The predicted variation in scaling of the thickness of the polymer shell with the degree of polymerization. Source: Adapted from Choi et al. [373].



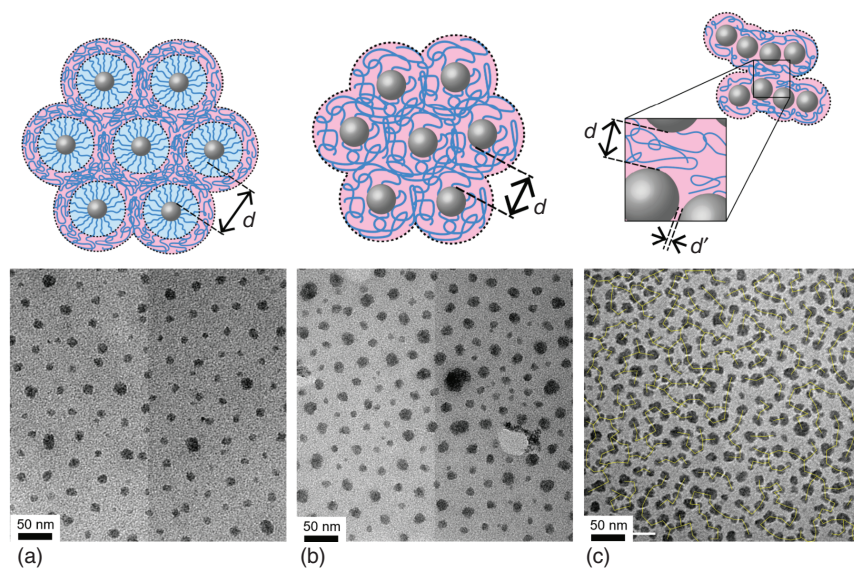
**Scheme 1.9** Schematic representation of the architecture of the grafted chains.

where  $N$  refers to the degree of polymerization, while in the SDPB regime, the scaling follows  $h \sim N^y$  ( $y = 3/5$  in good solvents). Besides, the performance of hairy nanoparticles is substantially affected by the chain architecture of the grafted polymer chains, Scheme 1.9. As one of the most versatile methods, SI-CRP has been applied to grow statistical/random [374], block [375, 376], gradient copolymers [377, 378], as well as hyperbranched [379, 380] and cyclic polymers [381–383] from various inorganic substrates.

Tuning the grafting density of the hairy nanoparticles can significantly impact their overall physicochemical properties [384–386]. Based on the modified DC theory, the critical degree of polymerization ( $N_c$ ) is defined where the grafted polymer ligands enter the SDPB regime from the CPB regime. The  $N_c$  value was determined by the surface curvature of the particle core as well as the grafting density of the hairy nanoparticles. As the polymer chains start to relax after the transition from CPB to SDPB regime, the properties of interparticle ligand entanglement and chain penetration can only occur in the SDPB regime [387]. Generally, the final grafting density of the hairy nanoparticle is determined by the density of initiating sites on the surface of nanoparticles, which is controlled during the surface functionalization step. A facile synthetic route to tune the concentration of ATRP initiating sites on the surface of silica nanoparticles is illustrated in Scheme 1.10. The mixture with different ratios of active and “dummy” anchoring ATRP initiators is applied to modulate the concentration of initiating sites and further the grafting density of the hairy nanoparticles [267, 389]. Additionally, in an alternative method, ATRP initiators can be partially removed through high-energy irradiation [390–392]. Hairy nanoparticles with densely grafted and intermediately grafted polymer shells exhibited uniform microstructures, while the sparsely grafted systems showed a string-like superstructure, Figure 1.7 [393]. One way to distinguish whether the hairy nanoparticles form uniform or string-like microstructures is to check



**Scheme 1.10** Synthesis of hairy nanoparticles with different grafting densities. Source: Reproduced from Wang et al. [388] with permission of American Chemical Society, Copyright 2020.

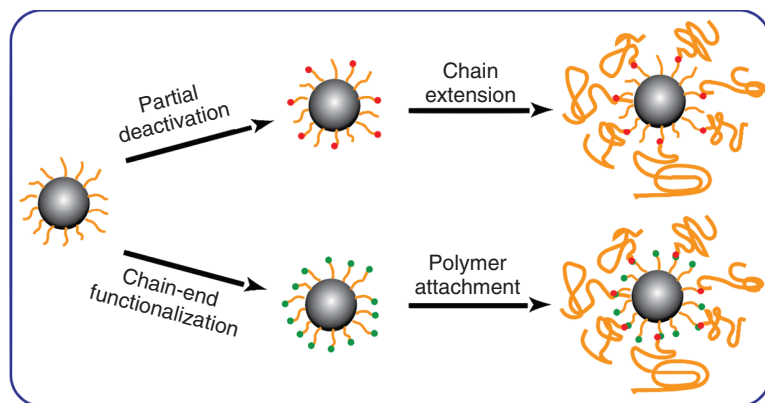


**Figure 1.7** Representative bright-field transmission electron micrographs for (a) dense ( $\text{SiO}_2$ -*d*-S365), (b) intermediate ( $\text{SiO}_2$ -*i*-S328), and (c) sparse ( $\text{SiO}_2$ -*s*-S432) PS-brush systems with similar degrees of polymerization. Also shown are schematic illustrations of the corresponding microstructures. Source: Lee et al. [393], Reproduced with permission of American Chemical Society.

their interparticle distance distributions through the image analysis performed on the TEM images. If the distance distribution is monomodal, the structure is considered uniform, which is attributed to the stronger hard-sphere-type attraction in densely/intermediately grafted hairy nanoparticle systems that promote the formation of highly ordered nanostructures, while a bimodal distribution suggests the formation of a string-like superstructure [373, 394–399].

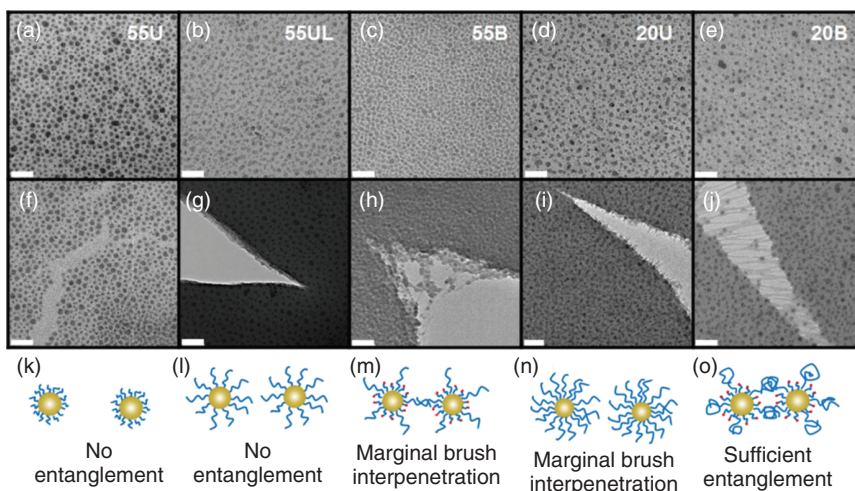
### 1.4.2 Bimodal Hairy Nanoparticles

A primary issue restraining the application of hairy nanoparticle solids is that short polymer ligands cannot afford sufficient chain entanglements for a tough material with good processibility, while high-molecular-weight ligands with the same grafting density significantly reduce the inorganic content and further the targeted improvements introduced by the inorganic nanofillers. Even though the inorganic fraction can maintain a decent value when applying sparsely grafted high molar mass polymer chains, the nontethered bare surface could result in severe agglomeration, which usually has detrimental effects on the performance of the material [400]. A possible solution to this dilemma was demonstrated by hairy nanoparticles with bimodal molecular weight distribution (Scheme 1.11) [401]. In an ideal case, the short polymer ligands densely cover the pristine nanoparticles without sacrificing the inorganic fraction to prevent the aggregation of nanoparticles. Meanwhile, as the transition from CPB to SDPB regime occurs at the chain ends of the short ligands, the introduction of sparsely grafted high molar mass ligands affords the chain entanglements for enhanced mechanical performance and processibility Figure 1.8.



**Scheme 1.11** Interactions of hairy nanoparticles with bimodal molecular weight distribution. Polymers with bimodal molecular weight distribution on hairy nanoparticles via “extending-from” (partial deactivation) strategy and “attaching-onto” (polymer attachment) strategy. Source: Reproduced from Yan et al. [401] with permission of American Chemical Society, Copyright 2015.

Bimodal block copolymer hairy nanoparticles with tunable assembling behavior were prepared using functionalized nanoparticles with different concentrations of



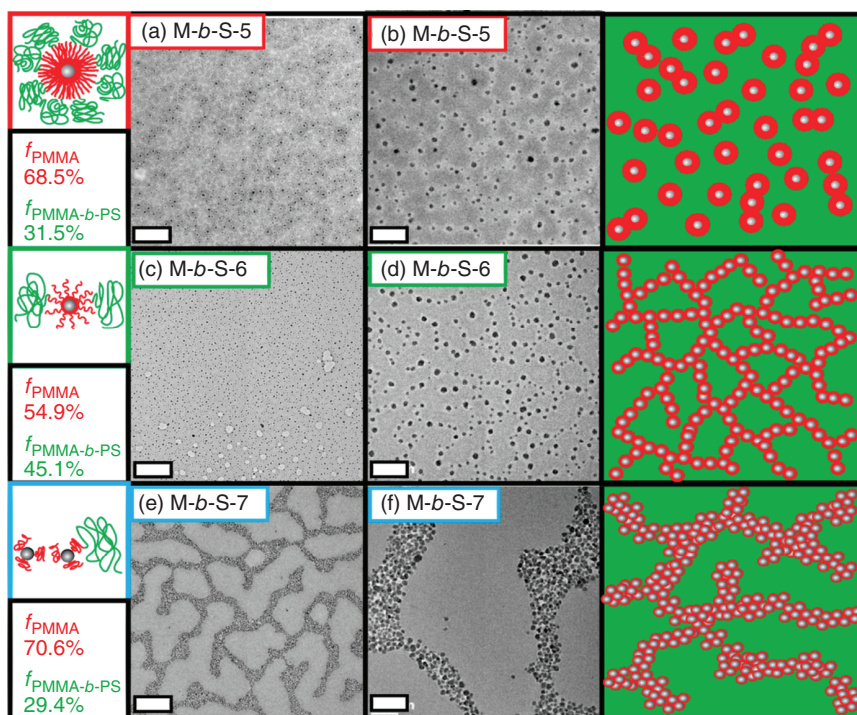
**Figure 1.8** TEM images of monolayers (a–e), crack formation (f–j), and illustrations of cracks (k–o) of the five  $\text{SiO}_2$ -*g*-PS hairy nanoparticles. Unimodal sample **55U** ( $\text{SiO}_2$ -*g*-PS<sub>80</sub>, a, f, k):  $N < N_e \sim 160$ , extensive crack propagation. Unimodal sample **55UL** ( $\text{SiO}_2$ -*g*-PS<sub>170</sub>, b, g, l): above entanglement limit but in CPB regime (DP < 250), sharp crack formation. Bimodal sample **55B** ( $\text{SiO}_2$ -*g*-*bi*-PS<sub>13,170</sub>, c, h, m): long brushes above entanglement limit and slightly beyond CPB–SDPB transition (grafting density  $\sim 0.11$  chains  $\text{nm}^{-2}$ ), plastic deformation. Unimodal sample **20U** ( $\text{SiO}_2$ -*g*-PS<sub>250</sub>, d, i, n):  $N > N_e$  and slightly beyond CPB–SDPB transition, stent-like undulation formation. Bimodal sample **20B** ( $\text{SiO}_2$ -*g*-*bi*-PS<sub>69,790</sub>, e, j, o): long brushes in SDPB regime and far above entanglement limit, craze formation. Scale bars = 100 nm. Source: Yan et al. [401], Reproduced with permission of American Chemical Society.

initiating sites. The primary PMMA blocks were extended with PS as the outer shell (Figure 1.9) [388]. The chain extension efficiency and bimodality of the grafting ligands were modulated by the concentration of hairy nanoparticle macroinitiators ( $\text{SiO}_2$ -*g*-PMMA-Br). Three different bimodal block copolymer hairy nanoparticles with densely/intermediately/sparsely grafted pristine PMMA blocks were synthesized. Due to their low extension efficiency, the three bimodal  $\text{SiO}_2$ -*g*-PMMA-*b*-PS hairy nanoparticles exhibited macroscopically uniform but microscopic string-like features, connected rings, and continuous cluster network morphologies, respectively. These observed different phase-separated structures were attributed to the segregation of PMMA- and PMMA-*b*-PS-grafted chains. This development offers a new path toward designing hierarchically ordered quasi-one-component materials.

## 1.5 Conclusion

The incorporation of inorganic nanofillers with polymers can achieve composites with overall enhanced performance and novel properties that are derived from the complex superposition of dynamics and interactions. Within the past decade, advancements in synthetic methodologies have enabled the preparation of hairy





**Figure 1.9** TEM images of bimodal  $\text{SiO}_2$ -*g*-PMMA-*b*-PS hairy nanoparticles. (a, b) densely grafted, (c, d) mediumly grafted, (e, f) sparsely grafted. Scale bar: (a), (c), (e), 500 nm; (b), (d), (f), 100 nm. Source: Wang et al. [388], Reproduced with permission of American Chemical Society.

nanoparticles with precisely engineered structures and compositions. Among the various approaches, SI-CRP is a robust technique that allows the synthesis of hairy nanoparticles with precise control over molar mass, dispersity, grafting density, the microstructure, as well as the architecture of the tethered chains. Although some recent reports present RAFT as a promising methodology to generate surface-grafted polymer chains, SI-ATRP is still the predominant technique in this field, mostly due to facile surface functionalization with ATRP initiators. It is possible to reduce the ATRP catalyst concentration to ppm level and reach a high conversion within a short reaction period with preserved chain-end fidelity. Besides, ATRP offers facile temporal and spatial control over the reaction through external stimuli, including photo-irradiation, electrical current, and ultrasound agitation. The major approaches to tether polymer ligands to inorganic substrates discussed in this chapter are “grafting-from” and “grafting-onto” methods. Generally, the “grafting-from” approach affords grafted polymer ligands with higher and tunable grafting densities; however, in this approach, a step of surface functionalization is needed before polymerization to introduce the initiating sites on the surface of nanoparticles. The “grafting-onto” approach does not always require the pre-treatment step, but due to the steric hindrance among the tether ligands, it is

difficult to achieve high grafting densities with this method. Subsequently, “ligand exchange” was developed to obtain high grafting densities with limited selections of interchangeable ligands.

The area of synthesis of hairy nanoparticles is among the most rapidly growing fields, as it provides access to previously unavailable novel materials for high-value potential applications, such as separation science, biosensors, non-fouling coatings, and organic electronics. Vast opportunities are predicted from the basic investigations toward large-scale, low-cost manufacturing of soft materials. Further research will focus on the expansion of the library of monomer selections applicable to SI-RDRP and the further advancement of chemical methods to understand the structure–property correlations and control higher-order chain characteristics, such as the sequence and the spatial distribution of repeat units along with the multicomponent graft systems. The opportunities for developing innovative material systems with better control of the microstructure could have a substantial impact on a broad range of soft matter technologies.

## Acknowledgment

This work is funded by the U.S. Department of Energy (DOE) Basic Energy Sciences (DE-SC00 18784).

## References

- 1 Ayres, N. (2010). *Polym. Chem.* 1 (6): 769–777.
- 2 Chen, T., Ferris, R., Zhang, J. et al. (2010). *Prog. Polym. Sci.* 35 (1): 94–112.
- 3 Galvin, C.J. and Genzer, J. (2012). *Prog. Polym. Sci.* 37 (7): 871–906.
- 4 Zoppe, J.O., Ataman, N.C., Mocny, P. et al. (2017). *Chem. Rev.* 117 (3): 1105–1318.
- 5 Krishnamoorthy, M., Hakobyan, S., Ramstedt, M., and Gautrot, J.E. (2014). *Chem. Rev.* 114 (21): 10976–11026.
- 6 Hui, C.M., Pietrasik, J., Schmitt, M. et al. (2014). *Chem. Mater.* 26 (1): 745–762.
- 7 Jiang, H. and Xu, F.-J. (2013). *Chem. Soc. Rev.* 42 (8): 3394–3426.
- 8 Zhao, B. and Zhu, L. (2009). *Macromolecules* 42 (24): 9369–9383.
- 9 Chen, T., Amin, I., and Jordan, R. (2012). *Chem. Soc. Rev.* 41 (8): 3280–3296.
- 10 Barbey, R., Lavanant, L., Paripovic, D. et al. (2009). *Chem. Rev.* 109 (11): 5437–5527.
- 11 Cayre, O.J., Chagneux, N., and Biggs, S. (2011). *Soft Matter* 7 (6): 2211–2234.
- 12 Bünsow, J., Kelby, T.S., and Huck, W.T.S. (2010). *Acc. Chem. Res.* 43 (3): 466–474.
- 13 Olivier, A., Meyer, F., Raquez, J.-M. et al. (2012). *Prog. Polym. Sci.* 37 (1): 157–181.
- 14 Xu, F.J., Neoh, K.G., and Kang, E.T. (2009). *Prog. Polym. Sci.* 34 (8): 719–761.
- 15 Hucknall, A., Rangarajan, S., and Chilkoti, A. (2009). *Adv. Mater.* 21 (23): 2441–2446.

- 16 Chen, H., Zhao, C., Zhang, M. et al. (2016). *Langmuir* 32 (14): 3315–3330.
- 17 Choudhury, S., Agrawal, A., Wei, S. et al. (2016). *Chem. Mater.* 28 (7): 2147–2157.
- 18 Sui, T., Song, B., Wen, Y.-h., and Zhang, F. (2016). *Sci. Rep.* 6 (1): 22696.
- 19 Kirillova, A., Schliebe, C., Stoychev, G. et al. (2015). *ACS Appl. Mater. Interfaces* 7 (38): 21218–21225.
- 20 Zhang, G., Allahyarov, E., and Zhu, L. (2018). Polymer nanodielectrics: current accomplishments and future challenges for electric energy storage. In: *Nano/Micro-Structured Materials for Energy and Biomedical Applications: Latest Developments, Challenges and Future Directions* (ed. B. Li and T. Jiao), 1–48. Singapore: Springer.
- 21 Miranda, O.R., Li, X., Garcia-Gonzalez, L. et al. (2011). *J. Am. Chem. Soc.* 133 (25): 9650–9653.
- 22 Ji, L., Lin, Z., Li, Y. et al. (2010). *Polymer* 51 (19): 4368–4374.
- 23 Kim, J.Y., Lee, B.S., Choi, J. et al. (2016). *Angew. Chem. Int. Ed.* 55 (49): 15306–15309.
- 24 Ma, H., Li, D., Sheng, X. et al. (2006). *Langmuir* 22 (8): 3751–3756.
- 25 Wang, D., Ye, G., Wang, X., and Wang, X. (2011). *Adv. Mater.* 23 (9): 1122–1125.
- 26 Hansoge, N.K. and Keten, S. (2019). *ACS Macro Lett.* 8 (10): 1209–1215.
- 27 Staszewski, T. (2020). *J. Phys. Chem. C* 124 (49): 27118–27129.
- 28 Dunderdale, G.J., Urata, C., Miranda, D.F., and Hozumi, A. (2014). *ACS Appl. Mater. Interfaces* 6 (15): 11864–11868.
- 29 Esparza-González, S.C., Sánchez-Valdés, S., Ramírez-Barrón, S.N. et al. (2016). *Toxicol. in Vitro* 37: 134–141.
- 30 Arfat, Y.A., Ahmed, J., Al Hazza, A. et al. (2017). *Int. J. Biol. Macromol.* 101: 1041–1050.
- 31 Matsuda, T. and Ohya, S. (2005). *Langmuir* 21 (21): 9660–9665.
- 32 Pietrasik, J., Bombalski, L., Cusick, B. et al. (2005). Controlling polymer chain topology and architecture by ATRP from flat surfaces. In: *Stimuli-Responsive Polymeric Films and Coatings*, ACS Symposium Series, vol. 912, 28–42. Washington: American Chemical Society.
- 33 Yan, J., Pan, X., Wang, Z. et al. (2016). *Macromolecules* 49 (23): 9283–9286.
- 34 Lee, H., Dellatore, S.M., Miller, W.M., and Messersmith, P.B. (2007). *Science* 318 (5849): 426–430.
- 35 Song, Y., Ye, G., Lu, Y. et al. (2016). *ACS Macro Lett.* 5 (3): 382–386.
- 36 Zeng, Z., Wen, M., Ye, G. et al. (2017). *Chem. Mater.* 29 (23): 10212–10219.
- 37 Zhou, L., Zheng, L., Yuan, J., and Wu, S. (2012). *Mater. Lett.* 78: 166–169.
- 38 Wang, Z., Mahoney, C., Yan, J. et al. (2016). *Langmuir* 32 (49): 13207–13213.
- 39 Yan, J., Pan, X., Wang, Z. et al. (2017). *Chem. Mater.* 29 (11): 4963–4969.
- 40 Zhang, J., Gu, P., Xu, J. et al. (2016). *Nanoscale* 8 (44): 18578–18595.
- 41 Wu, L., Zhang, Y., Yang, G. et al. (2016). *RSC Adv.* 6 (74): 69836–69844.
- 42 Leo, C.P., Cathie Lee, W.P., Ahmad, A.L., and Mohammad, A.W. (2012). *Sep. Purif. Technol.* 89: 51–56.
- 43 Khabibullin, A., Bhangaonkar, K., Mahoney, C. et al. (2016). *ACS Appl. Mater. Interfaces* 8 (8): 5458–5465.

- 44 Zeng, G., Liu, M., Shi, K. et al. (2016). *Appl. Surf. Sci.* 390: 710–717.
- 45 Zaborniak, I., Chmielarz, P., and Matyjaszewski, K. (2019). *Eur. Polym. J.* 120: 109253.
- 46 Basuki, J.S., Esser, L., Zetterlund, P.B. et al. (2013). *Macromolecules* 46 (15): 6038–6047.
- 47 Dong, H., Huang, J., Koepsel, R.R. et al. (2011). *Biomacromolecules* 12 (4): 1305–1311.
- 48 Matrab, T., Chehimi, M.M., Perruchot, C. et al. (2005). *Langmuir* 21 (10): 4686–4694.
- 49 Liu, T., Jia, S., Kowalewski, T. et al. (2003). *Langmuir* 19 (16): 6342–6345.
- 50 Böttcher, H., Hallensleben, M.L., Nuß, S. et al. (2002). *J. Mater. Chem.* 12 (5): 1351–1354.
- 51 Raula, J., Shan, J., Nuopponen, M. et al. (2003). *Langmuir* 19 (8): 3499–3504.
- 52 Dong, H., Zhu, M., Yoon, J.A. et al. (2008). *J. Am. Chem. Soc.* 130 (39): 12852–12853.
- 53 Kim, J.-B., Bruening, M.L., and Baker, G.L. (2000). *J. Am. Chem. Soc.* 122 (31): 7616–7617.
- 54 Mandal, T.K., Fleming, M.S., and Walt, D.R. (2002). *Nano Lett.* 2 (1): 3–7.
- 55 He, Q., Küller, A., Grunze, M., and Li, J. (2007). *Langmuir* 23 (7): 3981–3987.
- 56 Ohno, K., Koh, K.-m., Tsujii, Y., and Fukuda, T. (2002). *Macromolecules* 35 (24): 8989–8993.
- 57 Esteves, A.C.C., Bombalski, L., Trindade, T. et al. (2007). *Small* 3 (7): 1230–1236.
- 58 Kim, S.-W., Kim, S., Tracy, J.B. et al. (2005). *J. Am. Chem. Soc.* 127 (13): 4556–4557.
- 59 Yan, J., Bockstaller, M.R., and Matyjaszewski, K. (2020). *Prog. Polym. Sci.* 100: 101180–101230.
- 60 Acres, R.G., Ellis, A.V., Alvino, J. et al. (2012). *J. Phys. Chem. C* 116 (10): 6289–6297.
- 61 Ryu, J.H., Messersmith, P.B., and Lee, H. (2018). *ACS Appl. Mater. Interfaces* 10 (9): 7523–7540.
- 62 Connor, P.A., Dobson, K.D., and McQuillan, A.J. (1995). *Langmuir* 11 (11): 4193–4195.
- 63 Liebscher, J., Mrówczyński, R., Scheidt, H.A. et al. (2013). *Langmuir* 29 (33): 10539–10548.
- 64 Lynge, M.E., van der Westen, R., Postma, A., and Städler, B. (2011). *Nanoscale* 3 (12): 4916–4928.
- 65 Pranantyo, D., Xu, L.Q., Neoh, K.-G. et al. (2015). *Biomacromolecules* 16 (3): 723–732.
- 66 Kuang, J. and Messersmith, P.B. (2012). *Langmuir* 28 (18): 7258–7266.
- 67 Allara, D.L. and Nuzzo, R.G. (1985). *Langmuir* 1 (1): 45–52.
- 68 Zhang, L., He, R., and Gu, H.-C. (2006). *Appl. Surf. Sci.* 253 (5): 2611–2617.
- 69 Sun, S., Murray, C.B., Weller, D. et al. (2000). *Science* 287 (5460): 1989–1992.
- 70 Leff, D.V., Brandt, L., and Heath, J.R. (1996). *Langmuir* 12 (20): 4723–4730.

- 71 Kumar, A., Mandal, S., Selvakannan, P.R. et al. (2003). *Langmuir* 19 (15): 6277–6282.
- 72 Wu, N., Fu, L., Su, M. et al. (2004). *Nano Lett.* 4 (2): 383–386.
- 73 Zhang, J., Lee, J., Wang, Z. et al. (2017). *Polymer* 126: 126–132.
- 74 Armes, S.P., Gottesfeld, S., Beery, J.G. et al. (1991). *Polymer* 32 (13): 2325–2330.
- 75 Maeda, S., Corradi, R., and Armes, S.P. (1995). *Macromolecules* 28 (8): 2905–2911.
- 76 Jung, N., Kwon, S., Lee, D. et al. (2013). *Adv. Mater.* 25 (47): 6854–6858.
- 77 Sahoo, Y., Pizem, H., Fried, T. et al. (2001). *Langmuir* 17 (25): 7907–7911.
- 78 Burkett, S.L., Ko, N., Stern, N.D. et al. (2006). *Chem. Mater.* 18 (21): 5137–5143.
- 79 Tsubokawa, N. (1992). *Prog. Polym. Sci.* 17 (3): 417–470.
- 80 Delamar, M., Hitmi, R., Pinson, J., and Saveant, J.M. (1992). *J. Am. Chem. Soc.* 114 (14): 5883–5884.
- 81 Iruthayaraj, J., Chernyy, S., Lillethorup, M. et al. (2011). *Langmuir* 27 (3): 1070–1078.
- 82 Li, Y. and Zuilhof, H. (2012). *Langmuir* 28 (12): 5350–5359.
- 83 Colavita, P.E., Sun, B., Tse, K.-Y., and Hamers, R.J. (2007). *J. Am. Chem. Soc.* 129 (44): 13554–13565.
- 84 Leff, D.V., Ohara, P.C., Heath, J.R., and Gelbart, W.M. (1995). *J. Phys. Chem.* 99 (18): 7036–7041.
- 85 Templeton, A.C., Wuelfing, W.P., and Murray, R.W. (2000). *Acc. Chem. Res.* 33 (1): 27–36.
- 86 Grönbeck, H., Curioni, A., and Andreoni, W. (2000). *J. Am. Chem. Soc.* 122 (16): 3839–3842.
- 87 Xue, Y.-Q., Di, J.-M., Luo, Y. et al. (2014). *Oxid. Med. Cell. Longevity* 2014: 765832.
- 88 Desmet, T., Morent, R., De Geyter, N. et al. (2009). *Biomacromolecules* 10 (9): 2351–2378.
- 89 Chu, P.K., Chen, J.Y., Wang, L.P., and Huang, N. (2002). *Mater. Sci. Eng. R* 36 (5): 143–206.
- 90 Hu, S., Ren, X., Bachman, M. et al. (2002). *Anal. Chem.* 74 (16): 4117–4123.
- 91 Makamba, H., Kim, J.H., Lim, K. et al. (2003). *Electrophoresis* 24 (21): 3607–3619.
- 92 France, R.M. and Short, R.D. (1997). *J. Chem. Soc., Faraday Trans.* 93 (17): 3173–3178.
- 93 Wood, T.J. and Badyal, J.P.S. (2012). *ACS Appl. Mater. Interfaces* 4 (3): 1675–1682.
- 94 Siow, K.S., Britcher, L., Kumar, S., and Griesser, H.J. (2006). *Plasma Processes Polym.* 3 (6, 7): 392–418.
- 95 Khelifa, F., Ershov, S., Habibi, Y. et al. (2016). *Chem. Rev.* 116 (6): 3975–4005.
- 96 Teare, D.O.H., Barwick, D.C., Schofield, W.C.E. et al. (2005). *Langmuir* 21 (24): 11425–11430.
- 97 Kumar, R., Welle, A., Becker, F. et al. (2018). *ACS Appl. Mater. Interfaces* 10 (38): 31965–31976.

- 98 Coad, B.R., Styan, K.E., and Meagher, L. (2014). *ACS Appl. Mater. Interfaces* 6 (10): 7782–7789.
- 99 Han, J., Zhai, Y., Wang, Z. et al. (2020). *ACS Macro Lett.* 9 (9): 1218–1223.
- 100 Kumar, S.K., Benicewicz, B.C., Vaia, R.A., and Winey, K.I. (2017). *Macromolecules* 50 (3): 714–731.
- 101 Zhao, B. and Brittain, W.J. (2000). *Prog. Polym. Sci.* 25 (5): 677–710.
- 102 Edmondson, S., Osborne, V.L., and Huck, W.T.S. (2004). *Chem. Soc. Rev.* 33 (1): 14–22.
- 103 Ding, H., Yan, J., Wang, Z. et al. (2016). *Polymer* 107: 492–502.
- 104 Gao, H. and Matyjaszewski, K. (2007). *J. Am. Chem. Soc.* 129 (20): 6633–6639.
- 105 Möller, M., Künstle, H., and Kunz, M. (1991). *Synth. Met.* 41 (3): 1159–1162.
- 106 Zhang, Y., Wang, Z., Matyjaszewski, K., and Pietrasik, J. (2019). *Eur. Polym. J.* 110: 49–55.
- 107 Yuan, J., Xu, Y., Walther, A. et al. (2008). *Nat. Mater.* 7 (9): 718–722.
- 108 Müllner, M., Yuan, J., Weiss, S. et al. (2010). *J. Am. Chem. Soc.* 132 (46): 16587–16592.
- 109 Djalali, R., Li, S.-Y., and Schmidt, M. (2002). *Macromolecules* 35 (11): 4282–4288.
- 110 Pang, X., Zhao, L., Han, W. et al. (2013). *Nat. Nanotechnol.* 8 (6): 426–431.
- 111 Binder, W.H. (2019). *Macromol. Rapid Commun.* 40 (1): 1800610.
- 112 Laible, R. and Hamann, K. (1975). *Angew. Makromol. Chem.* 48 (1): 97–133.
- 113 Laible, R. and Hamann, K. (1980). *Adv. Colloid Interface Sci.* 13 (1): 65–99.
- 114 Prucker, O. and Rühle, J. (1998). *Macromolecules* 31 (3): 592–601.
- 115 M. Karahasanoğlu; A. Onen; I. Serhatm. *Prog. Org. Coat.* 2014, 77, 1079–1084.  
M. Karahasanoğlu, A. Önen, İ.E. Serhatlı
- 116 Ahin, M., Krawczyk, K., Roszkowski, P. et al. (2018). *Eur. Polym. J.* 98: 430–438.
- 117 Lee, H., Ryu, J., Kim, M. et al. (2016). *Radiat. Phys. Chem.* 125: 160–164.
- 118 Kang, Y., Choi, S.-H., Gopalan, A. et al. (2006). *J. Non-Cryst. Solids* 352: 463–468.
- 119 Woodworth, B.E., Metzner, Z., and Matyjaszewski, K. (1998). *Macromolecules* 31 (23): 7999–8004.
- 120 Pyun, J. and Matyjaszewski, K. (2001). *Chem. Mater.* 13 (10): 3436–3448.
- 121 Ohno, K., Morinaga, T., Koh, K. et al. (2005). *Macromolecules* 38 (6): 2137–2142.
- 122 Matyjaszewski, K., Miller, P.J., Pyun, J. et al. (1999). *Macromolecules* 32 (20): 6526–6535.
- 123 Matyjaszewski, K. (2012). *Macromolecules* 45 (10): 4015–4039.
- 124 Matyjaszewski, K. and Xia, J. (2001). *Chem. Rev.* 101 (9): 2921–2990.
- 125 Matyjaszewski, K. and Tsarevsky, N.V. (2014). *J. Am. Chem. Soc.* 136 (18): 6513–6533.
- 126 Wang, J.-S. and Matyjaszewski, K. (1995). *Macromolecules* 28 (23): 7901–7910.
- 127 Ejaz, M., Yamamoto, S., Ohno, K. et al. (1998). *Macromolecules* 31 (17): 5934–5936.
- 128 Bombalski, L., Min, K., Dong, H. et al. (2007). *Macromolecules* 40 (21): 7429–7432.

- 129 Ribelli, T.G., Lorandi, F., Fantin, M., and Matyjaszewski, K. (2019). *Macromol. Rapid Commun.* 40 (1): 1800616.
- 130 Jakubowski, W. and Matyjaszewski, K. (2006). *Angew. Chem. Int. Ed.* 45 (27): 4482–4486.
- 131 Jakubowski, W., Min, K., and Matyjaszewski, K. (2006). *Macromolecules* 39 (1): 39–45.
- 132 Konkolewicz, D., Wang, Y., Krys, P. et al. (2014). *Polym. Chem.* 5 (15): 4396–4417.
- 133 Konkolewicz, D., Wang, Y., Zhong, M. et al. (2013). *Macromolecules* 46 (22): 8749–8772.
- 134 Matyjaszewski, K., Jakubowski, W., Min, K. et al. (2006). *Proc. Natl. Acad. Sci. U.S.A.* 103 (42): 15309–15314.
- 135 Pan, X., Fantin, M., Yuan, F., and Matyjaszewski, K. (2018). *Chem. Soc. Rev.* 47 (14): 5457–5490.
- 136 Magenau, A.J.D., Strandwitz, N.C., Gennaro, A., and Matyjaszewski, K. (2011). *Science* 332 (6025): 81–84.
- 137 Chmielarz, P., Fantin, M., Park, S. et al. (2017). *Prog. Polym. Sci.* 69: 47–78.
- 138 Kwak, Y. and Matyjaszewski, K. (2010). *Macromolecules* 43 (12): 5180–5183.
- 139 Pan, X., Tasdelen, M.A., Laun, J. et al. (2016). *Prog. Polym. Sci.* 62: 73–125.
- 140 Wang, Z., Pan, X., Li, L. et al. (2017). *Macromolecules* 50 (20): 7940–7948.
- 141 Wang, Z., Pan, X., Yan, J. et al. (2017). *ACS Macro Lett.* 6 (5): 546–549.
- 142 Wang, Z., Wang, Z., Pan, X. et al. (2018). *ACS Macro Lett.* 7 (3): 275–280.
- 143 Wang, Z., Lorandi, F., Fantin, M. et al. (2019). *ACS Macro Lett.* 8 (2): 161–165.
- 144 Matyjaszewski, K., Wei, M., Xia, J., and McDermott, N.E. (1997). *Macromolecules* 30 (26): 8161–8164.
- 145 Dadashi-Silab, S., Pan, X., and Matyjaszewski, K. (2017). *Macromolecules* 50 (20): 7967–7977.
- 146 Pan, X., Malhotra, N., Dadashi-Silab, S., and Matyjaszewski, K. (2017). *Macromol. Rapid Commun.* 38 (13): 1600651.
- 147 Kato, M., Kamigaito, M., Sawamoto, M., and Higashimura, T. (1995). *Macromolecules* 28 (5): 1721–1723.
- 148 Ando, T., Kato, M., Kamigaito, M., and Sawamoto, M. (1996). *Macromolecules* 29 (3): 1070–1072.
- 149 Fors, B.P. and Hawker, C.J. (2012). *Angew. Chem. Int. Ed.* 51 (35): 8850–8853.
- 150 Treat, N.J., Sprafke, H., Kramer, J.W. et al. (2014). *J. Am. Chem. Soc.* 136 (45): 16096–16101.
- 151 Pan, X., Lamson, M., Yan, J., and Matyjaszewski, K. (2015). *ACS Macro Lett.* 4 (2): 192–196.
- 152 Pan, X., Fang, C., Fantin, M. et al. (2016). *J. Am. Chem. Soc.* 138 (7): 2411–2425.
- 153 Pan, X., Lathwal, S., Mack, S. et al. (2017). *Angew. Chem. Int. Ed.* 56 (10): 2740–2743.
- 154 Yan, J., Li, B., Zhou, F., and Liu, W. (2013). *ACS Macro Lett.* 2 (7): 592–596.
- 155 Li, B., Yu, B., Huck, W.T.S. et al. (2013). *J. Am. Chem. Soc.* 135 (5): 1708–1710.
- 156 Treat, N.J., Fors, B.P., Kramer, J.W. et al. (2014). *ACS Macro Lett.* 3 (6): 580–584.

- 157 Sato, T., Dunderdale, G.J., Urata, C., and Hozumi, A. (2018). *Macromolecules* 51 (24): 10065–10073.
- 158 Li, B., Yu, B., Huck, W.T.S. et al. (2012). *Angew. Chem. Int. Ed.* 51 (21): 5092–5095.
- 159 Poelma, J.E., Fors, B.P., Meyers, G.F. et al. (2013). *Angew. Chem. Int. Ed.* 52 (27): 6844–6848.
- 160 Min, K., Gao, H., and Matyjaszewski, K. (2007). *Macromolecules* 40 (6): 1789–1791.
- 161 Gnanou, Y. and Hizal, G. (2004). *J. Polym. Sci., Part A: Polym. Chem.* 42 (2): 351–359.
- 162 Kwak, Y., Magenau, A.J.D., and Matyjaszewski, K. (2011). *Macromolecules* 44 (4): 811–819.
- 163 Dong, H. and Matyjaszewski, K. (2008). *Macromolecules* 41 (19): 6868–6870.
- 164 Matyjaszewski, K., Dong, H., Jakubowski, W. et al. (2007). *Langmuir* 23 (8): 4528–4531.
- 165 Yan, W., Dadashi-Silab, S., Matyjaszewski, K. et al. (2020). *Macromolecules* 53 (8): 2801–2810.
- 166 Yan, W., Fantin, M., Ramakrishna, S. et al. (2019). *ACS Appl. Mater. Interfaces* 11 (30): 27470–27477.
- 167 Yan, W., Fantin, M., Spencer, N.D. et al. (2019). *ACS Macro Lett.* 8 (7): 865–870.
- 168 Fantin, M., Ramakrishna, S.N., Yan, J. et al. (2018). *Macromolecules* 51 (17): 6825–6835.
- 169 Dehghani, E.S., Du, Y., Zhang, T. et al. (2017). *Macromolecules* 50 (6): 2436–2446.
- 170 Wang, Y., Soerensen, N., Zhong, M. et al. (2013). *Macromolecules* 46 (3): 683–691.
- 171 Pietrasik, J., Dong, H., and Matyjaszewski, K. (2006). *Macromolecules* 39 (19): 6384–6390.
- 172 Dong, H., Tang, W., and Matyjaszewski, K. (2007). *Macromolecules* 40 (9): 2974–2977.
- 173 Mueller, L., Jakubowski, W., Tang, W., and Matyjaszewski, K. (2007). *Macromolecules* 40 (18): 6464–6472.
- 174 Tang, W., Tsarevsky, N.V., and Matyjaszewski, K. (2006). *J. Am. Chem. Soc.* 128 (5): 1598–1604.
- 175 Krys, P. and Matyjaszewski, K. (2017). *Eur. Polym. J.* 89: 482–523.
- 176 Matyjaszewski, K., Tsarevsky, N.V., Braunecker, W.A. et al. (2007). *Macromolecules* 40 (22): 7795–7806.
- 177 Zhang, Y., Wang, Y., and Matyjaszewski, K. (2011). *Macromolecules* 44 (4): 683–685.
- 178 Williams, V.A., Ribelli, T.G., Chmielarz, P. et al. (2015). *J. Am. Chem. Soc.* 137 (4): 1428–1431.
- 179 Yan, J., Pan, X., Schmitt, M. et al. (2016). *ACS Macro Lett.* 5 (6): 661–665.
- 180 Magenau, A.J.D., Bortolamei, N., Frick, E. et al. (2013). *Macromolecules* 46 (11): 4346–4353.
- 181 Chmielarz, P., Yan, J., Krys, P. et al. (2017). *Macromolecules* 50 (11): 4151–4159.



- 182 Ribelli, T.G., Konkolewicz, D., Bernhard, S., and Matyjaszewski, K. (2014). *J. Am. Chem. Soc.* 136 (38): 13303–13312.
- 183 Mosnáček, J. and Ilčíková, M. (2012). *Macromolecules* 45 (15): 5859–5865.
- 184 Konkolewicz, D., Schröder, K., Buback, J. et al. (2012). *ACS Macro Lett.* 1 (10): 1219–1223.
- 185 Anastasaki, A., Nikolaou, V., Zhang, Q. et al. (2014). *J. Am. Chem. Soc.* 136 (3): 1141–1149.
- 186 Xu, J., Jung, K., Atme, A. et al. (2014). *J. Am. Chem. Soc.* 136 (14): 5508–5519.
- 187 Ohtsuki, A., Goto, A., and Kaji, H. (2013). *Macromolecules* 46 (1): 96–102.
- 188 Anastasaki, A., Nikolaou, V., Simula, A. et al. (2014). *Macromolecules* 47 (12): 3852–3859.
- 189 Alfredo, N.V., Jalapa, N.E., Morales, S.L. et al. (2012). *Macromolecules* 45 (20): 8135–8146.
- 190 Xu, J., Jung, K., and Boyer, C. (2014). *Macromolecules* 47 (13): 4217–4229.
- 191 Dadashi-Silab, S., Atilla Tasdelen, M., and Yagci, Y. (2014). *J. Polym. Sci., Part A: Polym. Chem.* 52 (20): 2878–2888.
- 192 Discekici, E.H., Pester, C.W., Treat, N.J. et al. (2016). *ACS Macro Lett.* 5 (2): 258–262.
- 193 Theriot, J.C., Lim, C.-H., Yang, H. et al. (2016). *Science* 352 (6289): 1082–1086.
- 194 Ottou, W.N., Sardon, H., Mecerreyes, D. et al. (2016). *Prog. Polym. Sci.* 56: 64–115.
- 195 Mohapatra, H., Kleiman, M., and Esser-Kahn, A.P. (2017). *Nat. Chem.* 9 (2): 135–139.
- 196 Chiefari, J., Chong, Y.K., Ercole, F. et al. (1998). *Macromolecules* 31 (16): 5559–5562.
- 197 Perrier, S. and Takolpuckdee, P. (2005). *J. Polym. Sci., Part A: Polym. Chem.* 43 (22): 5347–5393.
- 198 Moad, G., Rizzardo, E., and Thang, S.H. (2005). *Aust. J. Chem.* 58 (6): 379–410.
- 199 Loiseau, J., Doërr, N., Suau, J.M. et al. (2003). *Macromolecules* 36 (9): 3066–3077.
- 200 Moad, G., Chong, Y.K., Postma, A. et al. (2005). *Polymer* 46 (19): 8458–8468.
- 201 Xu, J., Jung, K., Corrigan, N.A., and Boyer, C. (2014). *Chem. Sci.* 5 (9): 3568–3575.
- 202 McKenzie, T.G., Colombo, E., Fu, Q. et al. (2017). *Angew. Chem. Int. Ed.* 56 (40): 12302–12306.
- 203 Wang, Y., Fantin, M., Park, S. et al. (2017). *Macromolecules* 50 (20): 7872–7879.
- 204 Lv, C., He, C., and Pan, X. (2018). *Angew. Chem. Int. Ed.* 57 (30): 9430–9433.
- 205 Lee, H.J., Nakayama, Y., and Matsuda, T. (1999). *Macromolecules* 32 (21): 6989–6995.
- 206 Tsujii, Y., Ejaz, M., Sato, K. et al. (2001). *Macromolecules* 34 (26): 8872–8878.
- 207 Baum, M. and Brittain, W.J. (2002). *Macromolecules* 35 (3): 610–615.
- 208 Li, C. and Benicewicz, B.C. (2005). *Macromolecules* 38 (14): 5929–5936.
- 209 Peng, Q., Lai, D.M.Y., Kang, E.T., and Neoh, K.G. (2006). *Macromolecules* 39 (16): 5577–5582.
- 210 Zhao and Perrier, S. (2006). *Macromolecules* 39 (25): 8603–8608.

- 211 Ohno, K., Ma, Y., Huang, Y. et al. (2011). *Macromolecules* 44 (22): 8944–8953.
- 212 Li, C., Han, J., Ryu, C.Y., and Benicewicz, B.C. (2006). *Macromolecules* 39 (9): 3175–3183.
- 213 Khani, M.M., Abbas, Z.M., and Benicewicz, B.C. (2017). *J. Polym. Sci., Part A: Polym. Chem.* 55 (9): 1493–1501.
- 214 Niu, J., Lunn, D.J., Pusuluri, A. et al. (2017). *Nat. Chem.* 9 (6): 537–545.
- 215 Bagheri, A., Arandiyani, H., Adnan, N.N.M. et al. (2017). *Macromolecules* 50 (18): 7137–7147.
- 216 Demirci, S. and Caykara, T. (2012). *React. Funct. Polym.* 72 (9): 588–595.
- 217 Kitano, H., Liu, Y., Tokiwa, K.-i. et al. (2012). *Eur. Polym. J.* 48 (11): 1875–1882.
- 218 Kondo, T., Gemmei-Ide, M., Kitano, H. et al. (2012). *Colloids Surf., B* 91: 215–218.
- 219 Matsuzaka, N., Takahashi, H., Nakayama, M. et al. (2012). *J. Biomater. Sci., Polym. Ed.* 23 (10): 1301–1314.
- 220 Takahashi, H., Matsuzaka, N., Nakayama, M. et al. (2012). *Biomacromolecules* 13 (1): 253–260.
- 221 Takahashi, H., Nakayama, M., Itoga, K. et al. (2011). *Biomacromolecules* 12 (5): 1414–1418.
- 222 Bain, E.D., Dawes, K., Özçam, A.E. et al. (2012). *Macromolecules* 45 (9): 3802–3815.
- 223 Yu, H.-Y., Li, W., Zhou, J. et al. (2009). *J. Membr. Sci.* 343 (1): 82–89.
- 224 Zhou, J., Li, W., Gu, J.-S. et al. (2010). *Sep. Purif. Technol.* 71 (2): 233–240.
- 225 Macdonald, T., Gibson, C.T., Constantopoulos, K. et al. (2012). *Appl. Surf. Sci.* 258 (7): 2836–2843.
- 226 Islam, M.R., Bach, L.G., Vo, T.-S. et al. (2013). *Appl. Surf. Sci.* 286: 31–39.
- 227 Dilag, J., Kobus, H., and Ellis, A.V. (2013). *Forensic Sci. Dermatol. Int.* 228 (1): 105–114.
- 228 Grande, C.D., Tria, M.C., Jiang, G. et al. (2011). *Macromolecules* 44 (4): 966–975.
- 229 Tria, M.C.R., Grande, C.D.T., Ponnampati, R.R., and Advincula, R.C. (2010). *Biomacromolecules* 11 (12): 3422–3431.
- 230 Zengin, A. and Caykara, T. (2012). *J. Polym. Sci., Part A: Polym. Chem.* 50 (21): 4443–4450.
- 231 Jiao, Y. and Akcora, P. (2014). *J. Polym. Sci., Part A: Polym. Chem.* 52 (12): 1700–1705.
- 232 Wilczewska, A.Z. and Markiewicz, K.H. (2014). *Macromol. Chem. Phys.* 215 (2): 190–197.
- 233 Tian, J., Zheng, F., and Zhao, H. (2011). *J. Phys. Chem. C* 115 (8): 3304–3312.
- 234 Zengin, A., Yildirim, E., Tamer, U., and Caykara, T. (2013). *Analyst* 138 (23): 7238–7245.
- 235 Ye, Y.-S., Chen, Y.-N., Wang, J.-S. et al. (2012). *Chem. Mater.* 24 (15): 2987–2997.
- 236 Choi, J., Schattling, P., Jochum, F.D. et al. (2012). *J. Polym. Sci., Part A: Polym. Chem.* 50 (19): 4010–4018.
- 237 Di Carlo, G., Damin, F., Armelao, L. et al. (2012). *Appl. Surf. Sci.* 258 (8): 3750–3756.

- 238 Duan, Z., Qu, Z., Hu, F. et al. (2014). *Appl. Surf. Sci.* 300: 104–110.
- 239 Rotzoll, R. and Vana, P. (2008). *J. Polym. Sci., Part A: Polym. Chem.* 46 (23): 7656–7666.
- 240 Günay, K.A., Schüwer, N., and Klok, H.-A. (2012). *Polym. Chem.* 3 (8): 2186–2192.
- 241 Moraes, J., Ohno, K., Maschmeyer, T., and Perrier, S. (2013). *Chem. Mater.* 25 (17): 3522–3527.
- 242 Gurbuz, N., Demirci, S., Yavuz, S., and Caykara, T. (2011). *J. Polym. Sci., Part A: Polym. Chem.* 49 (2): 423–431.
- 243 Hua, D., Tang, J., Jiang, J. et al. (2009). *Mater. Chem. Phys.* 114 (1): 402–406.
- 244 Zengin, A., Karakose, G., and Caykara, T. (2013). *Eur. Polym. J.* 49 (10): 3350–3358.
- 245 Zhu, L.-J., Zhu, L.-P., Jiang, J.-H. et al. (2014). *J. Membr. Sci.* 451: 157–168.
- 246 Matsuzaka, N., Nakayama, M., Takahashi, H. et al. (2013). *Biomacromolecules* 14 (9): 3164–3171.
- 247 Hong, C.-Y., Li, X., and Pan, C.-Y. (2009). *J. Mater. Chem.* 19 (29): 5155–5160.
- 248 Dukes, D., Li, Y., Lewis, S. et al. (2010). *Macromolecules* 43 (3): 1564–1570.
- 249 Maillard, D., Kumar, S.K., Rungta, A. et al. (2011). *Nano Lett.* 11 (11): 4569–4573.
- 250 Huang, X., Appelhans, D., Formanek, P. et al. (2012). *ACS Nano* 6 (11): 9718–9726.
- 251 Huang, X., Appelhans, D., Formanek, P. et al. (2011). *Macromolecules* 44 (21): 8351–8360.
- 252 Moll, J.F., Akcora, P., Rungta, A. et al. (2011). *Macromolecules* 44 (18): 7473–7477.
- 253 Wang, L. and Benicewicz, B.C. (2013). *ACS Macro Lett.* 2 (2): 173–176.
- 254 Yang, K., Huang, X., Huang, Y. et al. (2013). *Chem. Mater.* 25 (11): 2327–2338.
- 255 Xu, L., Pan, J., Xia, Q. et al. (2012). *J. Phys. Chem. C* 116 (48): 25309–25318.
- 256 Xiong, L., Wang, R., Liang, H. et al. (2010). *J. Macromol. Sci. A* 47 (9): 903–908.
- 257 Demirci, S. and Caykara, T. (2012). *J. Polym. Sci., Part A: Polym. Chem.* 50 (15): 2999–3007.
- 258 Moad, G. and Rizzardo, E. (1995). *Macromolecules* 28 (26): 8722–8728.
- 259 Rizzardo, E., Serelis, A., and Solomon, D. (1982). *Aust. J. Chem.* 35 (10): 2013–2024.
- 260 Hawker, C.J., Barclay, G.G., Orellana, A. et al. (1996). *Macromolecules* 29 (16): 5245–5254.
- 261 Hawker, C.J. (1997). *Acc. Chem. Res.* 30 (9): 373–382.
- 262 Hawker, C.J., Bosman, A.W., and Harth, E. (2001). *Chem. Rev.* 101 (12): 3661–3688.
- 263 Studer, A. and Schulte, T. (2005). *Chem. Rec.* 5 (1): 27–35.
- 264 Ghannam, L., Parvole, J., Laruelle, G. et al. (2006). *Polym. Int.* 55 (10): 1199–1207.
- 265 Bartholome, C., Beyou, E., Bourgeat-Lami, E. et al. (2003). *Macromolecules* 36 (21): 7946–7952.

- 266 Parvole, J., Laruelle, G., Guimon, C. et al. (2003). *Macromol. Rapid Commun.* 24 (18): 1074–1078.
- 267 Husseman, M., Malmström, E.E., McNamara, M. et al. (1999). *Macromolecules* 32 (5): 1424–1431.
- 268 Parvole, J., Billon, L., and Montfort, J.P. (2002). *Polym. Int.* 51 (10): 1111–1116.
- 269 Ghannam, L., Bacou, M., Garay, H. et al. (2004). *Polymer* 45 (21): 7035–7045.
- 270 Blas, H., Save, M., Boissière, C. et al. (2011). *Macromolecules* 44 (8): 2577–2588.
- 271 Szwarc, M., Levy, M., and Milkovich, R. (1956). *J. Am. Chem. Soc.* 78 (11): 2656–2657.
- 272 Higashimura, T., Mitsuhashi, M., and Sawamoto, M. (1979). *Macromolecules* 12 (2): 178–182.
- 273 Matyjaszewski, K. (1996). *Cationic Polymerizations : Mechanisms, Synthesis, and Applications*. New York: Marcel Dekker.
- 274 Advincula, R., Zhou, Q., Park, M. et al. (2002). *Langmuir* 18 (22): 8672–8684.
- 275 Zhao, B. and Brittain, W.J. (2000). *Macromolecules* 33 (2): 342–348.
- 276 Spange, S., Simon, F., Schutz, H. et al. (1992). *J. Macromol. Sci. A* 29 (11): 997–1006.
- 277 Whitesell, J.K. and Chang, H.K. (1993). *Science* 261 (5117): 73–76.
- 278 Schmidt, A.M. (2005). *Macromol. Rapid Commun.* 26 (2): 93–97.
- 279 Carrot, G., Rutot-Houzé, D., Pottier, A. et al. (2002). *Macromolecules* 35 (22): 8400–8404.
- 280 Choi, I.S. and Langer, R. (2001). *Macromolecules* 34 (16): 5361–5363.
- 281 Schneider, M., Fetsch, C., Amin, I. et al. (2013). *Langmuir* 29 (23): 6983–6988.
- 282 Tsubokawa, N., Funaki, A., Hada, Y., and Sone, Y. (1982). *J. Polym. Sci. Polym. Chem.* 20 (12): 3297–3304.
- 283 Jordan, R. and Ulman, A. (1998). *J. Am. Chem. Soc.* 120 (2): 243–247.
- 284 Jordan, R., West, N., Ulman, A. et al. (2001). *Macromolecules* 34 (6): 1606–1611.
- 285 Calderon, N. (1972). *J. Macromol. Sci. C* 7 (1): 105–159.
- 286 Bielawski, C.W. and Grubbs, R.H. (2007). *Prog. Polym. Sci.* 32 (1): 1–29.
- 287 Schrock, R.R. (1990). *Acc. Chem. Res.* 23 (5): 158–165.
- 288 Grubbs, R. and Tumas, W. (1989). *Science* 243 (4893): 907–915.
- 289 Leitgeb, A., Wappel, J., and Slugovc, C. (2010). *Polymer* 51 (14): 2927–2946.
- 290 Slugovc, C. (2004). *Macromol. Rapid Commun.* 25 (14): 1283–1297.
- 291 Lynde, B.E., Maust, R.L., Li, P. et al. (2020). *Mater. Chem. Front.* 4 (1): 252–256.
- 292 Tallon, M.A. (2016). Ring-opening metathesis polymerization (ROMP) using maleic anhydride-based monomers. In: *Handbook of Maleic Anhydride Based Materials: Syntheses, Properties and Applications* (ed. O.M. Musa), 311–398. Berlin: Springer International Publishing.
- 293 LaNasa, J.A. and Hickey, R.J. (2020). *Macromolecules* 53 (19): 8216–8232.
- 294 Kim, N.Y., Jeon, N.L., Choi, I.S. et al. (2000). *Macromolecules* 33 (8): 2793–2795.
- 295 Ogawa, K.A., Goetz, A.E., and Boydston, A.J. (2015). *J. Am. Chem. Soc.* 137 (4): 1400–1403.
- 296 Mastan, E., Xi, L., and Zhu, S. (2016). *Macromol. Theory Simul.* 25 (3): 220–228.
- 297 Chevigny, C., Dalmas, F., Di Cola, E. et al. (2011). *Macromolecules* 44 (1): 122–133.

- 298 Hayashi, S., Handa, S., Oshibe, Y. et al. (1995). *Polym. J.* 27 (6): 623–630.
- 299 Yakushiji, T., Sakai, K., Kikuchi, A. et al. (1998). *Langmuir* 14 (16): 4657–4662.
- 300 Tsubokawa, N. and Kogure, A. (1991). *J. Polym. Sci., Part A: Polym. Chem.* 29 (5): 697–702.
- 301 Hosoya, H., Kumazaki, H., Chida, K. et al. (1990). *Pure Appl. Chem.* 62 (3): 445–450.
- 302 Lowe, A.B., Sumerlin, B.S., Donovan, M.S., and McCormick, C.L. (2002). *J. Am. Chem. Soc.* 124 (39): 11562–11563.
- 303 Rossner, C. and Vana, P. (2014). *Angew. Chem. Int. Ed.* 53 (46): 12639–12642.
- 304 Tao, P., Viswanath, A., Schadler, L.S. et al. (2011). *ACS Appl. Mater. Interfaces* 3 (9): 3638–3645.
- 305 Leophairatana, P., Samanta, S., De Silva, C.C., and Koberstein, J.T. (2017). *J. Am. Chem. Soc.* 139 (10): 3756–3766.
- 306 Golas, P.L. and Matyjaszewski, K. (2010). *Chem. Soc. Rev.* 39 (4): 1338–1354.
- 307 Lutz, J.-F., Börner, H.G., and Weichenhan, K. (2006). *Macromolecules* 39 (19): 6376–6383.
- 308 Golas, P.L. and Matyjaszewski, K. (2007). *QSAR Comb. Sci.* 26 (11, 12): 1116–1134.
- 309 Yoshimoto, K., Hirase, T., Madsen, J. et al. (2009). *Macromol. Rapid Commun.* 30 (24): 2136–2140.
- 310 Yavuz, M.S., Cheng, Y., Chen, J. et al. (2009). *Nat. Mater.* 8 (12): 935–939.
- 311 Julthongpiput, D., Lin, Y.-H., Teng, J. et al. (2003). *Langmuir* 19 (19): 7832–7836.
- 312 Huang, J., Koepsel, R.R., Murata, H. et al. (2008). *Langmuir* 24 (13): 6785–6795.
- 313 Costa, A.C., Geoghegan, M., Vlček, P., and Composto, R.J. (2003). *Macromolecules* 36 (26): 9897–9904.
- 314 Auschra, C., Eckstein, E., Mühlebach, A. et al. (2002). *Prog. Org. Coat.* 45 (2): 83–93.
- 315 Bulychiev, N.A., Arutunov, I.A., Zubov, V.P. et al. (2004). *Macromol. Chem. Phys.* 205 (18): 2457–2463.
- 316 Saleh, N., Sirk, K., Liu, Y.Q. et al. (2007). *Environ. Eng. Sci.* 24 (1): 45–57.
- 317 Saleh, N., Phenrat, T., Sirk, K. et al. (2005). *Nano Lett.* 5 (12): 2489–2494.
- 318 Saleh, N., Sarbu, T., Sirk, K. et al. (2005). *Langmuir* 21 (22): 9873–9878.
- 319 Wang, X.-S., Dykstra, T.E., Salvador, M.R. et al. (2004). *J. Am. Chem. Soc.* 126 (25): 7784–7785.
- 320 Dubois, F., Mahler, B., Dubertret, B. et al. (2007). *J. Am. Chem. Soc.* 129 (3): 482–483.
- 321 Sardar, R., Park, J.-W., and Shumaker-Parry, J.S. (2007). *Langmuir* 23 (23): 11883–11889.
- 322 Ehlert, S., Taheri, S.M., Pirner, D. et al. (2014). *ACS Nano* 8 (6): 6114–6122.
- 323 Wang, Z., Lu, Z., Mahoney, C. et al. (2017). *ACS Appl. Mater. Interfaces* 9 (8): 7515–7522.
- 324 Ding, H., Yan, J., Wang, Z. et al. (2017). *Polymer* 123: 392.
- 325 Zhao, Y., Wang, Z., Yuan, R. et al. (2018). *Polymer* 137: 370–377.

- 326 Moffitt, M., McMahon, L., Pessel, V., and Eisenberg, A. (1995). *Chem. Mater.* 7 (6): 1185–1192.
- 327 Chan, Y.N.C., Craig, G.S.W., Schrock, R.R., and Cohen, R.E. (1992). *Chem. Mater.* 4 (4): 885–894.
- 328 Ng Cheong Chan, Y., Schrock, R.R., and Cohen, R.E. (1992). *J. Am. Chem. Soc.* 114 (18): 7295–7296.
- 329 Park, J., Joo, J., Kwon, S.G. et al. (2007). *Angew. Chem. Int. Ed.* 46 (25): 4630–4660.
- 330 Möller, M., Spatz, J.P., and Roescher, A. (1996). *Adv. Mater.* 8 (4): 337–340.
- 331 Hess, P.H. and Parker, P.H. Jr., (1966). *J. Appl. Polym. Sci.* 10 (12): 1915–1927.
- 332 Thomas, J.R. (1966). *J. Appl. Phys.* 37 (7): 2914–2915.
- 333 Antonietti, M., Wenz, E., Bronstein, L., and Seregina, M. (1995). *Adv. Mater.* 7 (12): 1000–1005.
- 334 Burkett, S.L., Sims, S.D., and Mann, S. (1996). *Chem. Commun.* 11: 1367–1368.
- 335 Platonova, O.A., Bronstein, L.M., Solodovnikov, S.P. et al. (1997). *Colloid. Polym. Sci.* 275 (5): 426–431.
- 336 Seregina, M.V., Bronstein, L.M., Platonova, O.A. et al. (1997). *Chem. Mater.* 9 (4): 923–931.
- 337 Zhao, H., Douglas, E.P., Harrison, B.S., and Schanze, K.S. (2001). *Langmuir* 17 (26): 8428–8433.
- 338 Jaramillo, T.F., Baeck, S.-H., Cuenya, B.R., and McFarland, E.W. (2003). *J. Am. Chem. Soc.* 125 (24): 7148–7149.
- 339 Spatz, J.P., Mößmer, S., and Möller, M. (1996). *Chem. Eur. J.* 2 (12): 1552–1555.
- 340 Möller, M., Spatz, J.P., Roescher, A. et al. (1997). *Macromol. Symp.* 117 (1): 207–218.
- 341 Klingelhöfer, S., Heitz, W., Greiner, A. et al. (1997). *J. Am. Chem. Soc.* 119 (42): 10116–10120.
- 342 Warren, N.J. and Armes, S.P. (2014). *J. Am. Chem. Soc.* 136 (29): 10174–10185.
- 343 Charleux, B., Delaittre, G., Rieger, J., and D’Agosto, F. (2012). *Macromolecules* 45 (17): 6753–6765.
- 344 Wang, G., Schmitt, M., Wang, Z. et al. (2016). *Macromolecules* 49 (22): 8605–8615.
- 345 Wang, G., Wang, Z., Lee, B. et al. (2017). *Polymer* 129: 57–67.
- 346 Zhang, Y.-Y., Chen, C.-H., Xu, G.-C., and Xin, W.-B. (2019). *J. Mol. Struct.* 1176: 1–6.
- 347 Zhang, Y., Filipczak, P., He, G. et al. (2017). *Polymer* 129: 144–150.
- 348 Huang, J., Li, D., Liang, H., and Lu, J. (2017). *Macromol. Rapid Commun.* 38 (15): 1700202.
- 349 Wang, Z., Bockstaller, M.R., and Matyjaszewski, K. (2021). *ACS Mater. Lett.* 3 (5): 599–621.
- 350 Xie, G., Ding, H., Daniel, W.F.M. et al. (2016). *Polymer* 98: 481–486.
- 351 Adhikari, S., Nikoubashman, A., Leibler, L. et al. (2021). *ACS Polym. Au* 1 (1): 39–46.
- 352 Bilchak, C.R., Jhalalaria, M., Huang, Y. et al. (2020). *ACS Nano* 14 (12): 17174–17183.

- 353** Wang, Z., Chen, H., Wang, Y. et al. (2021). *ACS Appl. Mater. Interfaces* 13 (23): 27411–27418.
- 354** Wang, Z., Wang, Y., Chen, J. et al. (2021). *Langmuir* 37 (36): 10875–10881.
- 355** Adibnia, V., Mirbagheri, M., Faivre, J. et al. (2020). *Prog. Polym. Sci.* 110: 101298.
- 356** Faivre, J., Montembault, A., Sudre, G. et al. (2019). *Biomacromolecules* 20 (1): 326–335.
- 357** Seymour, B.T., Wright, R.A.E., Parrott, A.C. et al. (2017). *ACS Appl. Mater. Interfaces* 9 (29): 25038–25048.
- 358** Seymour, B.T., Fu, W., Wright, R.A.E. et al. (2018). *ACS Appl. Mater. Interfaces* 10 (17): 15129–15139.
- 359** Wright, R.A.E., Wang, K., Qu, J., and Zhao, B. (2016). *Angew. Chem. Int. Ed.* 55 (30): 8656–8660.
- 360** Bapat, A.P., Erck, R., Seymour, B.T. et al. (2018). *Eur. Polym. J.* 108: 38–47.
- 361** Fu, W., Bai, W., Jiang, S. et al. (2018). *Macromolecules* 51 (5): 1674–1680.
- 362** Xia, Y., Adibnia, V., Shan, C. et al. (2019). *Langmuir* 35 (48): 15535–15542.
- 363** Xia, Y., Adibnia, V., Huang, R. et al. (2019). *Angew. Chem. Int. Ed.* 58 (5): 1308–1314.
- 364** Jeong, W., Kang, H., Kim, E. et al. (2019). *Langmuir* 35 (41): 13268–13274.
- 365** Iqbal, D., Yan, J., Matyjaszewski, K., and Tilton, R.D. (2020). *Colloid. Polym. Sci.* 298 (1): 35–49.
- 366** Mai, W., Sun, B., Chen, L. et al. (2015). *J. Am. Chem. Soc.* 137 (41): 13256–13259.
- 367** Raj, W., Jerczynski, K., Rahimi, M. et al. (2021). *Mater. Sci. Eng. C* 130: 112439.
- 368** Reyes-Ortega, F., Parra-Ruiz, F.J., Averick, S.E. et al. (2013). *Polym. Chem.* 4 (9): 2800–2814.
- 369** Zhang, Y., Yan, J., Avellan, A. et al. (2020). *ACS Nano* 14 (9): 10954–10965.
- 370** Maynard, H.D., Heredia, K.L., Li, R.C. et al. (2007). *J. Mater. Chem.* 17 (38): 4015–4017.
- 371** Ohno, K., Morinaga, T., Takeno, S. et al. (2007). *Macromolecules* 40 (25): 9143–9150.
- 372** Daoud, M. and Cotton, J.P. (1982). *J. Phys. France* 43 (3): 531–538.
- 373** Choi, J., Hui, C.M., Schmitt, M. et al. (2013). *Langmuir* 29 (21): 6452–6459.
- 374** Ignatova, M., Voccia, S., Gilbert, B. et al. (2006). *Langmuir* 22 (1): 255–262.
- 375** Matyjaszewski, K., Miller, P.J., Shukla, N. et al. (1999). *Macromolecules* 32 (26): 8716–8724.
- 376** Pyun, J., Jia, S., Kowalewski, T. et al. (2003). *Macromolecules* 36 (14): 5094–5104.
- 377** Xu, C., Wu, T., Mei, Y. et al. (2005). *Langmuir* 21 (24): 11136–11140.
- 378** Wang, Z., Liu, T., Zhao, Y. et al. (2019). *Macromolecules* 52 (24): 9466–9475.
- 379** Mori, H., Seng, D.C., Zhang, M., and Müller, A.H.E. (2002). *Langmuir* 18 (9): 3682–3693.
- 380** Liu, P., Lu, W., Wang, W.-J. et al. (2012). Synthesis and characterization of PE-*b*-POEGMA copolymers prepared by linear/hyperbranched telechelic polyethylene-initiated ATRP of oligo(ethylene glycol) methacrylates. In: *Progress*

- in Controlled Radical Polymerization: Materials and Applications*, ACS Symposium Series, vol. 1101, 39–64. Washington: American Chemical Society.
- 381** Morgese, G., Trachsel, L., Romio, M. et al. (2016). *Angew. Chem. Int. Ed.* 55 (50): 15583–15588.
- 382** Morgese, G., Shirmardi Shaghasemi, B., Causin, V. et al. (2017). *Angew. Chem. Int. Ed.* 56 (16): 4507–4511.
- 383** Morgese, G., Cavalli, E., Rosenboom, J.-G. et al. (2018). *Angew. Chem. Int. Ed.* 57 (6): 1621–1626.
- 384** Saigal, T., Dong, H., Matyjaszewski, K., and Tilton, R.D. (2010). *Langmuir* 26 (19): 15200–15209.
- 385** Choi, J., Hui, C.M., Pietrasik, J. et al. (2012). *Soft Matter* 8 (15): 4072–4082.
- 386** Ojha, S., Beppler, B., Dong, H. et al. (2010). *Langmuir* 26 (16): 13210–13215.
- 387** Choi, J., Dong, H., Matyjaszewski, K., and Bockstaller, M.R. (2010). *J. Am. Chem. Soc.* 132 (36): 12537–12539.
- 388** Wang, Z., Lee, J., Wang, Z. et al. (2020). *ACS Macro Lett.* 9 (6): 806–812.
- 389** Tugulu, S. and Klok, H.-A. (2008). *Biomacromolecules* 9 (3): 906–912.
- 390** Yamamoto, S., Ejaz, M., Tsujii, Y., and Fukuda, T. (2000). *Macromolecules* 33 (15): 5608–5612.
- 391** Lin, C.Y., Marque, S.R.A., Matyjaszewski, K., and Coote, M.L. (2011). *Macromolecules* 44 (19): 7568–7583.
- 392** Tang, W., Kwak, Y., Braunecker, W. et al. (2008). *J. Am. Chem. Soc.* 130 (32): 10702–10713.
- 393** Lee, J., Wang, Z., Zhang, J. et al. (2020). *Macromolecules* 53 (4): 1502–1513.
- 394** Ohno, K., Morinaga, T., Takeno, S. et al. (2006). *Macromolecules* 39 (3): 1245–1249.
- 395** Chen, J., Fasoli, A., Cushen, J.D. et al. (2017). *Macromolecules* 50 (24): 9636–9646.
- 396** Voudouris, P., Choi, J., Dong, H. et al. (2009). *Macromolecules* 42 (7): 2721–2728.
- 397** Morinaga, T., Ohno, K., Tsujii, Y., and Fukuda, T. (2008). *Macromolecules* 41 (10): 3620–3626.
- 398** Ohno, K., Koh, K., Tsujii, Y., and Fukuda, T. (2003). *Angew. Chem. Int. Ed.* 42 (24): 2751–2754.
- 399** Nakanishi, Y., Ishige, R., Ogawa, H. et al. (2018). *J. Chem. Phys.* 148 (12): 124902.
- 400** Natarajan, B., Neely, T., Rungta, A. et al. (2013). *Macromolecules* 46 (12): 4909–4918.
- 401** Yan, J., Kristufek, T., Schmitt, M. et al. (2015). *Macromolecules* 48 (22): 8208–8218.